NACA

RESEARCH MEMORANDUM

GENERALIZED CHARTS FOR DETERMINATION OF PRESSURE DROP OF A HIGH-SPEED COMPRESSIBLE FLUID IN HEAT-EXCHANGER PASSAGES

I - AIR HEATED IN SMOOTH PASSAGES OF CONSTANT AREA WITH CONSTANT WALL TEMPERATURE

By Michael F. Valerino

Lewis Flight Propulsion Laboratory
Cleveland, Ohio

TECHNICAL EDITING WAIVED

NATIONAL ADVISORY COMMITTEE FOR AERONAUTICS

WASHINGTON
October 5, 1948

NACA RM No. E8G23

NATIONAL ADVISORY COMMITTEE FOR AERONAUTICS

RESEARCH MEMORANDUM

GENERALIZED CHARTS FOR DETERMINATION OF PRESSURE DROP OF A HIGH-SPEED COMPRESSIBLE FLUID IN HEAT-EXCHANGER PASSAGES

I - AIR HEATED IN SMOOTH PASSAGES OF CONSTANT AREA WITH CONSTANT WALL TEMPERATURE

By Michael F. Valerino

SUMMARY

The usual approximations made in calculating the pressure changes of a compressible fluid flowing through heat-exchanger passages introduce appreciable errors in the range of high-flow Mach numbers and high rates of heating. Existing methods for obtaining accurate results over the entire Mach number and rate-of-heating range require numerical integration for each specific set of conditions and are therefore too tedious for general application.

In the present paper an analysis is made of the compressible-flow variations occurring in heat-exchanger passages. The results of the analysis describe the flow and heating characteristics for which specific flow passages can be treated as segments of generalized flow systems. The graphical representation of the flow variations in the generalized flow systems can then be utilized as working charts to determine directly the pressure changes occurring in any specific flow passage. On the basis of these results, working charts are constructed to handle the case of air heated at constant wall temperature under turbulent-flow conditions. A method is given of incorporating the effect on the heat-exchanger flow process of high temperature differential between passage wall and fluid as based on recent NACA experimental data. Good agreement is obtained between the experimental and the chart pressure-drop values for passage-wall average temperatures as high as 1752° R (experimental limit) and for flow Mach numbers ranging from 0.32 to 1.00 (choke) at the passage exit.

INTRODUCTION

The rational design and calculation of performance of aircraft heat exchangers wherein heat is added to or subtracted from a high-speed compressible fluid stream requires not only the knowledge of the appropriate heat-transfer and friction-drag coefficients but also the mathematical means of utilizing these coefficients to describe accurately the pressure and temperature variations along the length of the heat-exchanger flow passage.

The basic differential equation describing the pressure variations of a compressible fluid under the simultaneous action of friction and heating or cooling is well known for the ideal case of one-dimensional flow; however, no exact closed-form solution of this differential-flow equation has yet been obtained even for specially chosen boundary conditions. Simplified solutions have been evolved (references 1 and 2) by resorting to approximations that are sufficiently valid for flow at relatively low speeds (corresponding to Mach numbers of the order of 0.4 and less) and for moderate rates of heat input to the fluid (corresponding to temperature differentials between wall and fluid of the order of 300° R and less). However, as illustrated by the experimental results of reference 3, the errors introduced by the approximations in calculating the pressure variations along a flow passage increase so rapidly with increase of Mach number and rate of heat input that for many heat-exchanger problems the simplified solutions are, at the most, only rough approximations.

Although the differential-flow equation is not susceptible to formal integration, it is readily amenable to numerical methods. Methods for numerically integrating the differential-flow equation for specific heat-exchanger conditions are discussed in references 4 and 5. Although the methods devised reduce the labor involved in obtaining numerical solutions it is desirable in the calculation of pressure drop to obviate the necessity for performing a numerical integration for each set of conditions of heat-exchanger operation.

In the present paper, an analysis of the heat-exchanger flow process is made that describes the generalization conditions for which specific flow passages can be treated as segments of generalized flow systems. The results of the analysis provide the basis for the construction of working charts that enable determination, without individual integration, of the pressure variations of a compressible fluid flowing through heat-exchanger passages.

Working charts are herein presented for the specific case of air flowing in turbulent motion through smooth constant-area passages wherein heat is added to the air stream by the passage walls which are at a constant temperature throughout their length. A constant ratio of the specific heats for air equal to 1.400 is used in the preparation of these charts. The range of variables covered in the charts are: (a) ratios of passage-wall temperature to air temperature (absolute) from 5.00 to 1.11, (b) total-momentum parameters equivalent to entrance Mach numbers from 0.15 to 0.80, and (c) passage length-diameter ratios from zero to a value sufficient in most cases to produce choking at the passage exit.

Although in the construction of the charts the heat-transfer coefficient and friction factor are expressed by the standard turbulent-flow equations used in present-day heat-exchanger work, a method is given for incorporating the effects of high temperature differential between passage wall and fluid on heat-transfer coefficient and friction factor as indicated by the recent experimental data of reference 6. A method of incorporating the experimental results of reference 6 in the heat-transfer relation used for temperature-rise calculation is also given. Calculated and measured values of pressure drop and temperature rise are compared.

An example is presented that illustrates in detail the method of using the working charts and of using the results of reference 6 in solution of a typical problem involving flow through a heat-exchanger passage. Application of the method of reference 5 for calculating the pressure changes of a compressible fluid flowing in a passage with an abrupt increase of cross section (as obtained at exit of heat exchanger) is discussed and illustrated.

Although of a preliminary nature, this paper is presented to fulfill the current urgent needs for this type of information.

SYMBOLS

A cross-sectional area of flow passage, (sq ft)

c_p specific heat of fluid at constant pressure, $\left(\text{Btu}/(\text{lb})(^\circ\text{R})\right)$

D_e equivalent diameter of flow passage, $\left(\frac{4A}{s}\right)$, (ft)

D_F drag force due to friction, (lb)

F friction factor, $\left(\frac{dp}{\frac{1}{2}\rho V^2 \frac{4\,dx}{D_e}}\right)$

f free-flow area ratio

g mass conversion factor, 32.2, (lb/slug)

h heat-transfer coefficient between wall and fluid, (Btu/(sec)(sq ft)(°R))

K_F ratio of actual value of friction factor to that given by the standard expression, $0.046 \left(\frac{\mu}{\rho g V D_e}\right)^{0.2}$

K_h ratio of actual value of heat-transfer coefficient to that given by the standard expression, $\frac{hD_e}{k} = 0.023 \left(\frac{\rho g V D_e}{\mu}\right)^{0.8} \left(\frac{c_p \mu}{k}\right)^{0.4}$

k thermal conductivity of fluid, (Btu/(sec)(sq ft)(°R)/(ft))

L passage flow length, (ft)

M Mach number

m mass flow of fluid, (slugs/sec)

P total pressure, (lb/sq ft absolute)

p static pressure, (lb/sq ft absolute)

R gas constant for fluid, (for air, equal to 53.35), (ft-lb/(lb)(°R))

s wetted perimeter, (ft)

T total temperature of fluid, (°R)

T_w temperature of passage walls, (°R)

t static temperature of fluid, (°R)

V fluid velocity in flow passage, (ft)/(sec)

x downstream distance from reference station in flow system, (ft)

Z parameter determined from table on charts

γ ratio of specific heats at total temperature of fluid (assumed constant as 1.400 in air charts)

μ viscosity of fluid, (lb)/(ft)(sec)

μ_r viscosity of air at 519° R, 12.3×10^{-6}, (lb)/(ft)(sec)

ρ mass density of fluid, (slugs/cu ft)

Subscripts:

av fluid conditions evaluated at average fluid temperature in flow passage

en entrance of given flow passage

ex exit of given flow passage

w fluid conditions evaluated at average wall temperature of flow passage

x any station in flow system

0 reference station, defined as station in flow system at which ratio $\frac{T_w}{T}$ is equal to any of values 5.0, 3.0, 2.0, or 1.5

The following groupings of variables are involved:

$mV+pA$ total momentum

$\frac{mV+pA}{m\sqrt{gRT}}$ total-momentum parameter

$\frac{pA}{m\sqrt{gRT}}$ static-pressure parameter

$\frac{PA}{m\sqrt{gRT}}$ total-pressure parameter

$\frac{V}{\sqrt{gRT}}$	velocity parameter
$\left(\frac{x}{D_e}\right)_{eff} = \left(\frac{\mu_{av}}{\mu_r}\right)^{0.2} (\rho V D_e)^{-0.2} K_F \frac{x}{D_e}$	effective length-diameter ratio as measured from reference station to any station in flow system
$\left(\frac{L}{D_e}\right)_{eff} = \left(\frac{\mu_{av}}{\mu_r}\right)^{0.2} (\rho V D_e)^{-0.2} K_F \frac{L}{D_e}$	effective length-diameter ratio of flow passage

ANALYSIS

The steady-flow process occurring within a constant-area heat-exchanger passage is one involving the simultaneous action of fluid friction and heat transfer. A general analysis is herein made of the compressible-flow variations obtained during this flow process. It is shown that, by appropriate limitations of the flow and heating conditions, individual flow processes become special cases of generalized flow systems; as a result generalized graphical representation of flow systems can be constructed that are applicable for the direct determination of the flow variations in a large number of different flow passages. The results of the analysis are then utilized for the construction of charts for air heated at constant wall temperature, assuming the standard heat-transfer and friction-factor equations for turbulent flow through smooth passages. A method of incorporating the effects of high temperature differential between passage wall and fluid on the flow process, as indicated by the recent experimental data of reference 6, is presented and checked with experiment.

For an over-all evaluation of heat-exchanger performance, the flow variations at the heat-exchanger entrance due to the flow-area contraction and at the heat-exchanger exit due to the flow-area enlargement must also be considered. Inasmuch as the entrance losses are usually small compared with the over-all losses across the heat exchanger, the flow process at the heat-exchanger entrance can generally be assumed isentropic. For a sharp-edge entrance, a more accurate determination of the pressure change in the flow

process at the heat-exchanger entrance can be obtained by subtracting the pressure drop due to the vena-contracta, as based on incompressible-flow considerations, from the pressure calculated for compressible isentropic flow. The losses at the heat-exchanger exit are usually of appreciable magnitude and require accurate evaluation. For this purpose, the analysis presented in reference 5 of the compressible-flow variations across a sudden enlargement is herein applied for the case of subsonic flow that is generally encountered in heat-exchanger practice.

Description of flow process. - One form of the differential-momentum equation describing the one-dimensional steady-state motion of a compressible fluid in a constant-area passage under the combined influence of friction and heat transfer is:

$$d(mV+pA) + dD_F = 0 \tag{1}$$

From the conservation of energy and mass equations and the perfect-gas law, reference 5 shows that the total-momentum parameter $\frac{mV+pA}{m\sqrt{gRT}}$ is uniquely related to each of the flow parameters M, $\frac{V}{\sqrt{gRT}}$, $\frac{pA}{m\sqrt{gRT}}$, $\frac{P}{p}$, and $\frac{T}{t}$ for any value of γ associated with the total temperature of the fluid. Knowledge of the variations of $\frac{mV+pA}{m\sqrt{gRT}}$ and T during the flow process is therefore sufficient to completely specify the variations of all the fluid-flow conditions (p, P, V, and t).

The variation of the total-momentum parameter $\frac{mV+pA}{m\sqrt{gRT}}$ is due to the variations of both the total-momentum mV+pA and the total temperature T. Differentiation of the total-momentum parameter with respect to these two variables for constant mass flow and area gives:

$$d\left(\frac{mV+pA}{m\sqrt{gRT}}\right) = \frac{d(mV+pA)}{m\sqrt{gRT}} - \frac{1}{2}\frac{mV+pA}{m\sqrt{gRT}}\frac{dT}{T} \tag{2}$$

The differential drag force dD_F is

$$dD_F = F\frac{1}{2}\rho V^2 A\frac{4\,dx}{D_e} \tag{3}$$

or, more conveniently,

$$dD_F = 2F\ mV\ d\left(\frac{x}{D_e}\right) \tag{4}$$

The variation of total temperature T is given by the differential relation equating the heat transferred from the wall to the fluid to the heat absorbed by the fluid.

$$mgc_p\ dT = hs\ (T_w-T)\ dx \tag{5}$$

The temperature recovery factor in the boundary layer is assumed to be unity in equation (5). Negligible errors are introduced by this assumption for gaseous fluids and for the practical range of temperature differentials used in heat exchangers.

Prandtl's extension of Reynold's analogy between fluid friction and heat transfer for flow through smooth-wall passages gives $\frac{\frac{h}{c_p\rho gV}}{\frac{F}{2}}$ as a function principally of the Prandtl number $\frac{c_p\mu}{k}$. In view of this relation, equation (5) is rearranged and presented as

$$dT = 2\left(\frac{\frac{h}{c_p\rho gV}}{\frac{F}{2}}\right)(T_w-T)\ F\ d\left(\frac{x}{D_e}\right) \tag{6}$$

From equations (1), (2), (4), and (6), the variation of the total-momentum parameter during the flow process is expressible as:

$$d\left(\frac{mV+pA}{m\sqrt{gRT}}\right) = -\frac{V}{\sqrt{gRT}}\frac{dT}{\left(\frac{\frac{h}{c_p\rho gV}}{\frac{F}{2}}\right)(T_w-T)} - \frac{1}{2}\frac{mV+pA}{m\sqrt{gRT}}\frac{dT}{T} \tag{7}$$

As previously pointed out, $\frac{mV+pA}{m\sqrt{gRT}}$ is related to $\frac{V}{\sqrt{gRT}}$ and T in the manner dictated by the laws of conservation of energy and mass, the perfect-gas law, and the relation between γ and T;

equation (7) thus involves only the variables $\frac{mV+pA}{m\sqrt{gRT}}$, $\frac{\frac{h}{c_p\rho gV}}{\frac{F}{2}}$, T_w, and T. The conclusion can then be drawn that for a given fluid the variation of $\frac{mV+pA}{m\sqrt{gRT}}$ during the flow process is uniquely determined by the variation of T during the process provided that $\frac{\frac{h}{c_p\rho gV}}{\frac{F}{2}}$ and T_w are constant or are expressible as functions of only $\frac{mV+pA}{m\sqrt{gRT}}$ and T. Because $\frac{mV+pA}{m\sqrt{gRT}}$ and T completely define all the fluid-flow conditions, the parallel generalization can be made that the flow variations of a fluid along a heat-exchanger passage are uniquely determined by the variation of T along the passage when the local values of $\frac{\frac{h}{c_p\rho gV}}{\frac{F}{2}}$ and T_w are constant or are expressible as functions of only the local fluid-flow conditions. In particular, the flow variations are then explicitly independent of the position variable x. Thus when the generalization conditions are satisfied, any station in a given flow system can be considered as the initial starting point of a real flow process; conversely, individual flow processes can be considered as special cases of generalized flow systems.

The results of integration of equations (6) and (7) for a number of generalized flow systems can be presented in chart form for the direct determination of the flow variations in a large number of individual flow passages when the generalization conditions are satisfied. This fact is used as the basis for the construction of the charts presented herein.

Pressure-drop charts for air heated at constant wall temperature. - Working charts were constructed on the basis of the foregoing analysis to enable determination, without individual integration, of the pressure variations sustained by air flowing through constant-area passages wherein heat is added to the air at constant passage-wall temperature. Conventional heat-transfer and friction relations were used in the preparation of the charts. Subsequent to the completion of the charts, additional data were obtained (reference 6) that indicate an effect of passage-wall temperature

on heat-transfer coefficient and friction factor that becomes important at high temperature differentials between wall and fluid. Hence, K_h and K_F are herein introduced as correction factors that account for departure of the actual heat-transfer and friction phenomena from the phenomena expressed by the conventional relations. The method of evaluating K_h and K_F in accordance with the recent data of reference 6 is reserved for a later section.

The relations and assumptions used in the integration of equations (6) and (7) are as follows:

(a) The ratio of the specific heats γ is taken constant as 1.400

(b) The relation for friction factor is taken as

$$F = 0.046 \left(\frac{\mu}{\rho g V D_e}\right)^{0.2} K_F \tag{8}$$

When $K_F = 1.00$, equation (8) reduces to the conventional relation (reference 7, p. 119, equation (9a)). Inasmuch as μ enters in F only to the 0.2 power, it is assumed constant in the integration of equation (6). Large variations in μ are accounted for in the use of the results by taking an average value of μ in the flow passage (that is, $\mu = \mu_{av}$). The factor K_F is also assumed constant in the integration of equation (6) and, as indicated later, is evaluated for the average fluid conditions existing in the flow passage.

(c) The relation for heat-transfer coefficient is taken as

$$\frac{hD_e}{k} = 0.023 \left(\frac{\rho g V D_e}{\mu}\right)^{0.8} \left(\frac{c_p \mu}{k}\right)^{0.4} K_h \tag{9}$$

When $K_h = 1.00$, equation (9) reduces to the conventional relation (reference 7, p. 168, equation (4c)).

From equations (8) and (9),

$$\frac{\frac{h}{c_p \rho g V}}{\frac{F}{2}} = \left(\frac{c_p \mu}{k}\right)^{-0.6} \frac{K_h}{K_F} \tag{10}$$

1004

The simplifications are made that: first, $\left(\frac{c_p\mu}{k}\right)^{-0.6}$ equals 1.186 which represents, within 1.5 percent, the value for air over the extreme temperature range 460° to 2500° R; and second, $\frac{K_h}{K_F}$ is equal to unity in accordance with Prandtl's extension of Reynold's analogy. Thus, $\frac{\frac{h}{c_p\rho gV}}{\frac{F}{2}}$ is taken constant as 1.186 in the integration of equations (6) and (7).

Two modes of heat addition of present interest are characterized by having (a) constant passage-wall temperature (T_w = a constant) and (b) constant rate of heat input along the passage length [$h(T_w-T)$ = a constant]. The generalization conditions are satisfied for both these modes of heat addition for the foregoing assumed heat-transfer and friction phenomena during the process; generalization is therefore possible. Only the case of constant passage-wall temperature is specifically treated herein.

For convenience of analysis and of presentation of results, the differential variable in equations (6) and (7) is changed from T to $\frac{T}{T_w}$. In the integration of equations (6) and (7), the lower integration limits are designated by the subscript 0. When equation (8) is substituted for F in equation (6) and μ is considered to be equal to μ_{av}, the parameter

$$\left(\frac{x}{D_e}\right)_{eff} = \left(\frac{\mu_{av}}{\mu_r}\right)^{0.2} (\rho V D_e)^{-0.2} K_F \frac{x}{D_e} \tag{11}$$

is introduced. This parameter, which is proportional to the product of the actual friction factor FK_F and the length-diameter ratio $\frac{x}{D_e}$, is of the same order of magnitude as $\frac{x}{D_e}$.

On the basis of the foregoing manipulations and assumptions, equation (6) can be formally integrated to give:

$$\left(\frac{T_w}{T}\right)_x = \frac{\left(\frac{T_w}{T}\right)_0}{\frac{T_x}{T_0}} \tag{12}$$

where

$$\frac{T_x}{T_0} = 1 + \left[\left(\frac{T_w}{T}\right)_0 - 1\right]\left[1 - e^{-0.00568\left(\frac{x}{D_e}\right)_{eff}}\right] \qquad (13)$$

Integration of equation (7) is numerically performed to give values of $\frac{mV+pA}{m\sqrt{gRT}}$ in one to one correspondence with values of $\frac{T_w}{T}$ for each assumed initial pair of values of $\left(\frac{mV+pA}{m\sqrt{gRT}}\right)_0$ and $\left(\frac{T_w}{T}\right)_0$. Inasmuch as the flow variations are explicitly independent of the position variable x, each corresponding pair of values of $\frac{T_w}{T}$ and $\frac{mV+pA}{m\sqrt{gRT}}$ obtained during a single integration [integration for one pair of values of $\left(\frac{mV+pA}{m\sqrt{gRT}}\right)_0$ and $\left(\frac{T_w}{T}\right)_0$] can be considered as the entrance conditions of a flow passage; thus each integration gives results for an infinite number of flow passages whose entrance conditions are restricted to the one-to-one relation between $\frac{mV+pA}{m\sqrt{gRT}}$ and $\frac{T_w}{T}$ obtained in the integration. All possible combinations of $\frac{mV+pA}{m\sqrt{gRT}}$ and $\frac{T_w}{T}$ that may be encountered in heat-exchanger practice are obtained if the integration of equation (7) is carried out for a single value of $\left(\frac{T_w}{T}\right)_0$ and a range of values of $\left(\frac{mV+pA}{m\sqrt{gRT}}\right)_0$. However, in order to obtain increased accuracy for the entire range of interest, the integration was actually carried out and is presented for four values of $\left(\frac{T_w}{T}\right)_0$. From the results of numerical integration of equation (7) and from equations (12) and (13), the values of $\frac{mV+pA}{m\sqrt{gRT}}$ in one-to-one correspondence with values of $\left(\frac{x}{D_e}\right)_{eff}$ for each value of $\left(\frac{T_w}{T}\right)_0$ and $\left(\frac{mV+pA}{m\sqrt{gRT}}\right)_0$ used in the integration are obtained. The plotting of these results in chart form is described later.

It is convenient in the use of the charts to recast equations (12) and (13) as follows:

Solution for $\left(\frac{x}{D_e}\right)_{eff}$ from equation (13) and substitution for $\frac{T_x}{T_0}$ from equation (12) gives for $x = x_{en}$, in which case subscript x is replaced by subscript en,

1004

$$\left(\frac{x_{en}}{D_e}\right)_{eff} = 176.1 \log_e \left\{ \frac{\left(\frac{T_w}{T}\right)_0 - 1}{\left(\frac{T_w}{T}\right)_0 \left[1 - \left(\frac{T}{T_w}\right)_{en}\right]} \right\} \tag{14}$$

Equation (13) is rewritten by substituting subscripts ex and en for x and 0, respectively, in which case x = L

$$\frac{T_{ex}}{T_{en}} = 1 + \left[\left(\frac{T_w}{T}\right)_{en} - 1\right]\left[1 - e^{-0.00568\left(\frac{L}{D_e}\right)_{eff}}\right] \tag{15}$$

Evaluation of K_h and K_F. - The preliminary heat-transfer and pressure-drop data of reference 6 are used to determine the average values of K_h and K_F that account for the effect of high temperature differentials between passage wall and fluid on the heat-transfer and pressure-loss phenomena in smooth-flow passages. These data were recently obtained at the NACA Cleveland laboratory in an investigation conducted with air flowing through a tube that was electrically heated to average wall temperatures of from 710° to 1700° R. Reference 6 shows that correlation of the heat-transfer data according to equation (9) wherein K_h was taken as unity and the physical properties c_p, μ, ρ, and k of the fluid were evaluated at the average bulk temperature resulted in a separation of the data as the temperature level of the wall varied. It was found, however, that satisfactory correlation of the heat-transfer data over the entire range of wall temperature is obtained by the equation:

$$\frac{hD_e}{k_w} = 0.022 \left(\frac{\rho_w g V D_e}{\mu_w}\right)^{0.8} \left(\frac{c_p \mu}{k}\right)_w^{0.4} \tag{16}$$

wherein

$$\rho_w V = (\rho V)\left(\frac{\rho_w}{\rho}\right) \tag{17}$$

Equation (16) can be rearranged as follows:

$$\frac{hD_e}{k} = 0.022\left(\frac{\rho g V D_e}{\mu}\right)^{0.8}\left(\frac{c_p\mu}{k}\right)^{0.4}\left[\left(\frac{\rho_w}{\rho}\right)^{0.8}\left(\frac{c_{p,w}}{c_p}\right)\left(\frac{\mu_w}{\mu}\right)^{0.2}\frac{\left(\frac{c_p\mu}{k}\right)^{0.6}}{\left(\frac{c_p\mu}{k}\right)_w^{0.6}}\right] \tag{18}$$

If $\frac{c_p\mu}{k}$ is assumed constant for air and if the simplification is made that ρ is inversely proportional to T rather than t, the average value of K_h in a flow passage is obtained from equations (9) and (18) as:

$$K_h = \frac{0.022}{0.023}\left(\frac{T_{av}}{T_w}\right)^{0.8}\left(\frac{c_{p,w}}{c_{p,av}}\right)\left(\frac{\mu_w}{\mu_{av}}\right)^{0.2} \tag{19}$$

The average values of T, μ, and c_p used in equation (19) are consistent with the determination of an average value of K_h for the flow passage.

The pressure-drop data of reference 6 are presently in the analysis stage; no definite conclusions have been reached regarding the effect of high temperature differentials between passage wall and fluid on friction factor. In the absence of such information it can be tentatively assumed that $\frac{\frac{h}{c_p\rho g V}}{\frac{F}{2}}$ remains substantially constant with variation of wall temperature. Therefore,

$$K_F = K_h \tag{20}$$

From substitution of equations (19) and (20) in equation (11) letting $x = L$, the effective length-diameter ratio of a flow passage can be expressed as

$$\left(\frac{L}{D_e}\right)_{eff} = \left(\frac{0.022}{0.023}\right)\left(\frac{T_{av}}{T_w}\right)^{0.8}\left(\frac{c_{p,w}}{c_{p,av}}\right)\left(\frac{\mu_w}{\mu_r}\right)^{0.2}(\rho V D_e)^{-0.2}\left(\frac{L}{D_e}\right) \tag{21}$$

In order to ascertain the validity of the assumption expressed by equation (20), a comparison was made, for several experimental runs, of the pressure drops measured in the investigation of reference 6 with the pressure drops obtained from the charts using equation (21) for evaluating the $\left(\frac{L}{D_e}\right)_{eff}$ of the experimental flow passage. Inasmuch as in the investigation the wall temperature varied with length along the tube, the integrated average value of T_w was used in the calculations. The results of the pressure-drop comparison as well as of a comparison of the calculated and measured temperature-rise values are presented in table I.

The good agreement between the measured and the calculated results indicated in the table substantiates the general validity of equations (19) and (20) and is a check on the accuracy of the charts and assumptions involved therein. In addition, the results of the foregoing comparison show that, although strictly applicable for the case of constant wall temperature, the charts can be used, within limits, to handle the case of nonuniform wall-temperature distribution along the passage length through the use of the average wall temperature. A measure of the nonuniformity of wall-temperature distribution is given by the ratio of the difference between maximum wall temperature and entrance-air temperature to the difference between average wall temperature and entrance-air temperature. For the runs used in the foregoing comparison this ratio was approximately 1.2.

At the relatively low Reynolds number of 53,600, the agreement is not as close as at the higher Reynolds numbers. This result is attributed to the laminar boundary-layer regime at the tube entrance which, because of the smooth well-rounded entry of the test tube, occupies an extensive portion of the tube length even for Reynolds numbers greatly in excess of the critical value. The extent of the entrance laminar regime is reduced with increase in Reynolds number.

The method of determining $\left(\frac{L}{D_e}\right)_{eff}$ for a flow passage is illustrated later by means of an example.

Flow in passage with sudden increase in cross section. - In reference 5, the momentum equation describing the flow of a compressible fluid across a sudden enlargement of cross section is written in terms of dimensionless-flow parameters for convenient application to the case where the flow in the passage just upstream

of the area enlargement is critical or supersonic. In heat-exchanger operation, however, the flow is generally subsonic; the general method of reference 5 is herein applied to this specific case.

For subsonic flow across a sudden enlargement (from area A_1 to area A_2), application of the principle of conservation of momentum at a section just downstream of the enlargement and at a section located a sufficient distance downstream of the enlargement that uniform flow again exists gives:

$$mV_1 + p_1A_2 = mV_2 + p_2A_2 \tag{22}$$

where

subscript 1 denotes conditions at the small area A_1

subscript 2 denotes conditions at the large area A_2

Because the mass flow and total temperature of the fluid are constant across the enlargement, equation (22) can be written

$$\left(\frac{mV+pA}{m\sqrt{gRT}}\right)_2 = \frac{mV_1+p_1A_2}{m\sqrt{gRT_1}} = \left(\frac{mV+pA}{m\sqrt{gRT}}\right)_1 + \frac{p_1\,(A_2-A_1)}{m\sqrt{gRT_1}} \tag{23}$$

or, more conveniently, when noting that $f = \frac{A_1}{A_2}$,

$$\left(\frac{mV+pA}{m\sqrt{gRT}}\right)_2 = \left(\frac{mV+pA}{m\sqrt{gRT}}\right)_1 + \left(\frac{pA}{m\sqrt{gRT}}\right)_1 \left(\frac{1}{f} - 1\right) \tag{24}$$

The use of equation (24) for calculation of the compressible-flow changes across an enlargement for subsonic flow is illustrated later by means of an example.

DESCRIPTION OF CHARTS

In figure 1, the ratio of the total momentum at any station to the total momentum at the reference station $\frac{(mV+pA)_x}{(mV+pA)_0}$ is plotted against the reciprocal of the total-momentum

parameter at the reference station $\left(\frac{m\sqrt{gRT}}{mV+pA}\right)_0$ for a range of values of effective length-diameter ratio $\left(\frac{x}{D_e}\right)_{eff}$. The ratio $\left(\frac{x}{D_e}\right)_{eff}$ is taken for the distance between the reference station and the station x in the flow system. Within each figure, the locus of all flow conditions in a given flow passage has one value of the abscissa. Hence, the points on a figure representing all flow conditions in a passage lie on a common vertical line. Each curve of constant $\left(\frac{x}{D_e}\right)_{eff}$ in figure 1 also represents the locus of points at which $\frac{T_w}{T}$ is a constant. Figure 1(a), which is for $\left(\frac{T_w}{T}\right)_0 = 5.0$, covers a range of $\left(\frac{x}{D_e}\right)_{eff}$ from 0 to 32.1 equivalent to a range of $\frac{T_w}{T}$ from 5.0 to 3.0; figure 1(b), which is for $\left(\frac{T_w}{T}\right)_0 = 3.0$, covers a range of $\left(\frac{x}{D_e}\right)_{eff}$ from 0 to 50.65 equivalent to a range of $\frac{T_w}{T}$ from 3.0 to 2.0; figure 1(c), which is for $\left(\frac{T_w}{T}\right)_0 = 2.0$, covers a range of $\left(\frac{x}{D_e}\right)_{eff}$ from 0 to 71.4 equivalent to a range of $\frac{T_w}{T}$ from 2.0 to 1.5; and figure 1(d), which is for $\left(\frac{T_w}{T}\right)_0 = 1.5$, covers a range of $\left(\frac{x}{D_e}\right)_{eff}$ from 0 to 208 equivalent to a range of $\frac{T_w}{T}$ from 1.5 to 1.11. Thus a total range of $\frac{T_w}{T}$ from 5.0 to 1.11 is covered in figure 1.

Inasmuch as the bottom curve in each of figures 1(a) to 1(c) is used in proceeding from one figure to another when required in solution of a problem, it is dashed and is identified with its appropriate value of $\frac{T_w}{T}$. These values are $\frac{T_w}{T} = 3.0$ obtained at $\left(\frac{x}{D_e}\right)_{eff} = 32.1$ in figure 1(a), $\frac{T_w}{T} = 2.0$ obtained at $\left(\frac{x}{D_e}\right)_{eff} = 50.65$ in figure 1(b), and $\frac{T_w}{T} = 1.5$ obtained at $\left(\frac{x}{D_e}\right)_{eff} = 71.4$ in figure 1(c). At $\left(\frac{x}{D_e}\right)_{eff} = 0$, $\frac{T_w}{T}$, of course, equals the value of $\left(\frac{T_w}{T}\right)_0$ for which the figure is presented. Because the value of $\frac{T_w}{T}$ corresponding to maximum $\left(\frac{x}{D_e}\right)_{eff}$

on a figure is identical with the reference value of $\frac{T_w}{T}$ on the succeeding figure, the maximum value of $\left(\frac{x}{D_e}\right)_{eff}$ in figures 1(a) to 1(c) represents the effective length-diameter ratio between the reference station for which the figure is presented and the reference station in the succeeding figure. For example, from figure 1(b), the $\left(\frac{x}{D_e}\right)_{eff}$ value between the reference station defined by $\left(\frac{T_w}{T}\right)_0 = 3.0$ and the reference station defined by $\left(\frac{T_w}{T}\right)_0 = 2.0$ is 50.65. The curve representing the choke limit for the flow is given in each figure. A table is presented in figures 1(a) to 1(c) that is useful, as later shown, in proceeding from one figure to another where required in the solution of a problem.

Figures 2 and 3 relate for air ($\gamma = 1.400$) the total-pressure parameter $\frac{PA}{m\sqrt{gRT}}$ and the static-pressure parameter $\frac{pA}{m\sqrt{gRT}}$, respectively, to the total-momentum parameter $\frac{mV+pA}{m\sqrt{gRT}}$. The variation of $\frac{mV+pA}{m\sqrt{gRT}}$ and T in a flow passage can therefore be translated into the variation of static or total pressure in the flow passage.

OPERATIONS INVOLVED IN USE OF CHARTS

The operations involved in the use of the charts for solution of a heat-exchanger flow problem are briefly outlined and illustrated in the following examples with the aid of figures 4 and 5. Figure 4 presents a schematic diagram of the flow passage of examples I, II, and III and indicates the passage (solid lines) as a segment of a generalized flow system shown by the dashed lines. The relative positions of the various stations in the generalized flow system that enter in the problem of example I are indicated. The detailed steps involved in the use of the charts for solution of the problem of example I are traced in figures 5(a), 5(b), and 5(c).

1004

Example I - Use of Charts

Consider the turbulent flow of air through a smooth tube wherein heat is added to the air at constant wall temperature. The following flow and heating conditions are assumed to exist:

(1) Equivalent diameter of tube, D_e, (ft) 0.0833
(2) Length of tube, L, (ft) 7
(3) Mass flow of air through tube, m, slugs/(sec) . . 0.00373
(4) Total temperature of air at tube entrance, T_{en}, $^{\circ}R$ 610
(5) Total pressure of air at tube entrance, P_{en}, (lb)/(sq ft) 2160
(6) Tube-wall temperature, T_w, $^{\circ}R$ 2000

Determine:

(a) Total pressure and total temperature of air at tube exit
(b) Static pressure of air at tube entrance and exit

The method of successive approximations is required to calculate the average value of $\left(\frac{L}{D_e}\right)_{eff}$ for the tube passage that is consistent with the average fluid temperature in the passage. Inasmuch as the principal purpose of this example is to illustrate the chart operations, the evaluation of $\left(\frac{L}{D_e}\right)_{eff}$, although the first step in obtaining solution of the problem, is presented later in example II.

(7) The results of example II give

$$\left(\frac{L}{D_e}\right)_{eff} = 103.0$$

(8) From items (4) and (6)

$$\left(\frac{T_w}{T}\right)_{en} = \frac{2000}{610} = 3.279$$

(9) From equation (15) and items (7) and (8)

$$\frac{T_{ex}}{T_{en}} = 1 + (3.279 - 1)\left(1 - e^{-0.00568 \times 103.0}\right) = 2.010$$

(10) From items (1) and (3)

$$\rho V = \frac{m}{A} = \frac{0.00373}{\frac{\pi}{4} \times (0.0833)^2} = 0.6837$$

(11) From items (4), (5), and (10) for R = 53.35 for air

$$\left(\frac{PA}{m\sqrt{gRT}}\right)_{en} = \frac{2160}{0.6837\sqrt{32.2 \times 53.35 \times 610}} = 3.087$$

(12) From item (11) and figure 2

$$\left(\frac{mV+pA}{m\sqrt{gRT}}\right)_{en} = 3.252$$

Determination of initial chart. - Items (8) and (12) specify the entrance conditions of the tube required for entering the charts. The point on the charts corresponding to the entrance conditions of the tube is referred to as the starting point and the chart containing the starting point as the initial chart. The initial chart is simply determined by the value of $\left(\frac{T_w}{T}\right)_{en}$ as illustrated in the following item.

(13) From item (8), $\left(\frac{T_w}{T}\right)_{en} = 3.279$; hence, figure 1(a) which covers the range $\frac{T_w}{T} = 5.0$ to 3.0 is the initial chart.

Inasmuch as consideration of several reference stations in the flow system may be required in solution of a problem, the reference station for which the initial chart is presented and all flow conditions at that reference station are designated by the subscript 0,1; for example, $\left(\frac{T_w}{T}\right)_{0,1}$ is equal to 5.0, the reference value on the initial chart. As shown in figure 4, reference station 0,1 in the flow system is located upstream of the flow-passage entrance (station en).

1004

Location of starting point on initial chart. -

(14) $\left(\frac{x_{en}}{D_e}\right)_{eff}$ is calculated from equation (14) for $\left(\frac{T_w}{T}\right)_{en} = 3.279$ (item (8)) and $\left(\frac{T_w}{T}\right)_0$ on the initial chart (designated as $\left(\frac{T_w}{T}\right)_{0,1}$ and equal to 5.0 from item (13)).

$$\left(\frac{x_{en}}{D_e}\right)_{eff} = 176.1 \log_e \left[\frac{5.0 - 1.0}{5.0\left(1 - \frac{1}{3.279}\right)}\right] = 24.76$$

As shown in figure 4, $\left(\frac{x_{en}}{D_e}\right)_{eff}$ represents the effective length-diameter ratio between stations 0,1 and en, that is, the effective length-diameter ratio required to effect a change in $\frac{T_w}{T}$ from 5.0 to 3.279.

(15) The ordinate-to-abscissa ratio on the initial chart for $x = x_{en}$ is

$$\frac{(mV+pA)_{en}}{(mV+pA)_{0,1}} \Bigg/ \left(\frac{m\sqrt{gRT}}{mV+pA}\right)_{0,1}$$

which, because T_w is constant, can be rewritten as

$$\left(\frac{mV+pA}{m\sqrt{gRT}}\right)_{en} \sqrt{\left(\frac{T}{T_w}\right)_{en}\left(\frac{T_w}{T}\right)_{0,1}}$$

This ratio, which represents the slope of a straight line through the origin of coordinates in the initial chart, is evaluated from items (8), (12), and (13) as

$$3.252\sqrt{\frac{5.0}{3.279}} = 4.013$$

Intersection of the straight line with slope 4.013 and the interpolated curve for $\left(\frac{x}{D_e}\right)_{eff} = \left(\frac{x_{en}}{D_e}\right)_{eff} = 24.76$ (item (14)) locates the starting point on the initial chart. Inasmuch as the origin of coordinates is not on the charts, the required slant line is obtained by drawing a straight line through the points (ordinate = 1.00, abscissa = 1/4.013) and (ordinate = 0.94, abscissa = 0.94/4.013). The foregoing construction procedure for location of the starting point is illustrated in figure 5(a) where the starting point is designated as point A.

(16) The ordinate value for the starting point is $\frac{(mV+pA)_{en}}{(mV+pA)_{0,1}}$, which is read from figure 1(a) as 0.990.

(17) The abscissa value for the starting point is $\left(\frac{m\sqrt{gRT}}{mV+pA}\right)_{0,1}$, which is read from figure 1(a) as 0.2467.

Determination of terminal chart. - The terminal chart is that chart containing the point corresponding to the exit conditions of the flow passage. This point is herein referred to as the end point and is designated as point D in figure 5(c). The terminal chart is determined as illustrated in items (18) and (19).

(18) The effective length-diameter ratio between reference station 0,1 and the end of the tube passage (station ex in fig. 4) is $\left(\frac{x_{en+L}}{D_e}\right)_{eff}$, which is simply the sum of $\left(\frac{x_{en}}{D_e}\right)_{eff}$ (item (14)) and the $\left(\frac{L}{D_e}\right)_{eff}$ of the tube passage (item (7)).

$$\left(\frac{x_{en+L}}{D_e}\right)_{eff} = 24.76 + 103.0 = 127.76$$

(19) The table presented on the initial chart (fig. 1(a), in this case) specifies the terminal chart as fig. 1(c) for the value $\left(\frac{x_{en+L}}{D_e}\right)_{eff}$ equal to 127.76.

Transfer from initial to terminal chart. - Inasmuch as the terminal chart is not the same as the initial chart, solution of

the problem requires transferring from chart to chart until the terminal chart is entered. In this case, it is necessary to transfer successively from figure 1(a) to figure 1(b) and finally to figure 1(c). In the performance of this transfer, the abscissa values required to enter figures 1(b) and 1(c) are successively determined as follows:

(20) On the initial chart, the ordinate corresponding to $\left(\frac{m\sqrt{gRT}}{mV+pA}\right)_{0,1}$ along the curve for maximum $\left(\frac{x}{D_e}\right)_{eff}$ is equal to $\frac{(mV+pA)_{0,2}}{(mV+pA)_{0,1}}$ where subscript 0,2 denotes the reference station at which $\left(\frac{T_w}{T}\right)_0 = \left(\frac{T_w}{T}\right)_{0,2}$ = the value of $\frac{T_w}{T}$ at maximum $\left(\frac{x}{D_e}\right)_{eff}$ on the initial chart. From figure 1(a) for item (17) and for $\left(\frac{x}{D_e}\right)_{eff}$ = 32.1 (maximum value),

$$\frac{(mV+pA)_{0,2}}{(mV+pA)_{0,1}} = 0.9862$$

where

$$\left(\frac{T_w}{T}\right)_{0,2} = 3.0$$

As indicated in figure (4), station 0,2 is the next successive reference station downstream of station 0,1. The point on the charts corresponding to the foregoing conditions is designated as point B in figure 5(a).

(21) The reciprocal of the total-momentum parameter at reference station 0,2 is calculated as

$$\left(\frac{m\sqrt{gRT}}{mV+pA}\right)_{0,2} = \left(\frac{m\sqrt{gRT}}{mV+pA}\right)_{0,1} \frac{(mV+pA)_{0,1}}{(mV+pA)_{0,2}} \sqrt{\left(\frac{T_w}{T}\right)_{0,1}\left(\frac{T}{T_w}\right)_{0,2}}$$

which from items (17) and (20) for $\left(\frac{T_w}{T}\right)_{0,1} = 5.0$ (item (13)) and $\left(\frac{T_w}{T}\right)_{0,2} = 3.0$ (item (20)), gives

$$\frac{0.2467}{0.9862}\sqrt{\frac{5.0}{3.0}} = 0.3229$$

The chart for $\left(\frac{T_w}{T}\right)_0 = \left(\frac{T_w}{T}\right)_{0,2} = 3.0$ (fig. 1(b)) is entered with an abscissa value equal to 0.3229 as indicated in figure 5(b). Inasmuch as figure 1(b) is not the terminal chart, the procedure of items (20) and (21) must be repeated.

(22) On the chart for $\left(\frac{T_w}{T}\right)_0 = \left(\frac{T_w}{T}\right)_{0,2}$, the ordinate corresponding to $\left(\frac{m\sqrt{gRT}}{mV+pA}\right)_{0,2}$ along the curve for maximum $\left(\frac{x}{D_e}\right)_{eff}$ is equal to $\frac{(mV+pA)_{0,3}}{(mV+pA)_{0,2}}$ where subscript 0,3 denotes the reference station at which $\left(\frac{T_w}{T}\right)_0 = \left(\frac{T_w}{T}\right)_{0,3}$ = the value of $\frac{T_w}{T}$ at maximum $\left(\frac{x}{D_e}\right)_{eff}$ on the chart. From figure 1(b) for item (21) and for $\left(\frac{x}{D_e}\right)_{eff} = 50.65$,

$$\frac{(mV+pA)_{0,3}}{(mV+pA)_{0,2}} = 0.9621$$

where $\left(\frac{T_w}{T}\right)_{0,3} = 2.0$.

As indicated in figure 4, station 0,3 is the next successive reference station downstream of station 0,2. The point on the charts corresponding to the foregoing conditions is designated as point C in figure 5(b).

(23) The reciprocal of the total-momentum parameter at reference station 0,3 is calculated as

$$\left(\frac{m\sqrt{gRT}}{mV+pA}\right)_{0,3} = \left(\frac{m\sqrt{gRT}}{mV+pA}\right)_{0,2} \frac{(mV+pA)_{0,2}}{(mV+pA)_{0,3}} \sqrt{\left(\frac{T_w}{T}\right)_{0,2} \left(\frac{T}{T_w}\right)_{0,3}}$$

which, from items (21) and (22) for $\left(\frac{T_w}{T}\right)_{0,2}$ = 3.0 (item (20)) and $\left(\frac{T_w}{T}\right)_{0,3}$ = 2.0 (item (22)), gives

$$\frac{0.3229}{0.9621}\sqrt{\frac{3.0}{2.0}} = 0.4111$$

The chart for $\left(\frac{T_w}{T}\right)_0 = \left(\frac{T_w}{T}\right)_{0,3}$ = 2.0 (fig. 1(c)) is entered with an abscissa value equal to 0.4111 as indicated in figure 5(c). Inasmuch as figure 1(c) is the terminal chart (item (19)), the transfer procedure is completed.

Location of end point on terminal chart. -

(24) The table presented on the initial chart (fig. 1(a), in this case) specifies Z = 82.75 for $\left(\frac{x_{en}+L}{D_e}\right)_{eff}$ = 127.76 (item (18)).

(25) The end point is located on the curve in the terminal chart for

$$\left(\frac{x}{D_e}\right)_{eff} = \left(\frac{x_{en}+L}{D_e}\right)_{eff} - Z$$

which, from items (18) and (25), gives

$$\left(\frac{x}{D_e}\right)_{eff} \text{ on terminal chart} = 127.76 - 82.75 = 45.01$$

(26) Items (23)and (25) fix the location of the end point on the terminal chart (fig. 1(c)); item (23) specifies the abscissa value for the end point as 0.4111 and item (25) specifies the

$\left(\frac{x}{D_e}\right)_{eff}$ value for the end point as 45.01. This procedure is illustrated in figure 5(c) where the end point is designated as point D.

Evaluation of $\left(\frac{mV+pA}{m\sqrt{gRT}}\right)_{ex}$. -

(27) Note that 3 charts, and thus 3 reference stations are involved in this problem for location of the end point. In this case, the ordinate value for the end point is

$$\frac{(mV+pA)_{ex}}{(mV+pA)_{0,3}}$$

which, from item (26), is read as 0.9463 in figure 1(c).

(28) $\frac{(mV+pA)_{ex}}{(mV+pA)_{0,1}}$ is calculated as

$$\frac{(mV+pA)_{ex}}{(mV+pA)_{0,1}} = \frac{(mV+pA)_{0,2}}{(mV+pA)_{0,1}} \frac{(mV+pA)_{0,3}}{(mV+pA)_{0,2}} \frac{(mV+pA)_{ex}}{(mV+pA)_{0,3}}$$

which, from items (20), (22), and (27), is

$$0.9862 \times 0.9621 \times 0.9463 = 0.8979$$

(29) $\frac{(mV+pA)_{ex}}{(mV+pA)_{en}}$ is calculated as

$$\frac{(mV+pA)_{ex}}{(mV+pA)_{en}} = \frac{(mV+pA)_{ex}}{(mV+pA)_{0,1}} \frac{(mV+pA)_{0,1}}{(mV+pA)_{en}}$$

which, from items (16) and (28), gives

$$\frac{(mV+pA)_{ex}}{(mV+pA)_{en}} = \frac{0.8979}{0.990} = 0.9069$$

(30) The total-momentum parameter at the exit of the flow passage is then

$$\left(\frac{mV+pA}{m\sqrt{gRT}}\right)_{ex} = \left(\frac{mV+pA}{m\sqrt{gRT}}\right)_{en} \frac{(mV+pA)_{ex}}{(mV+pA)_{en}} \sqrt{\frac{T_{en}}{T_{ex}}}$$

which, from items (9), (12), and (29), gives

$$\left(\frac{mV+pA}{m\sqrt{gRT}}\right)_{ex} = \frac{3.252 \times 0.9069}{\sqrt{2.010}} = 2.080$$

Final results. -

(31) From item (30) and figure 2(a)

$$\left(\frac{PA}{m\sqrt{gRT}}\right)_{ex} = 1.778$$

(32) From items (9), (11), and (31)

$$\frac{P_{ex}}{P_{en}} = \left(\frac{PA}{m\sqrt{gRT}}\right)_{ex} \left(\frac{m\sqrt{gRT}}{PA}\right)_{en} \sqrt{\frac{T_{ex}}{T_{en}}} = \frac{1.778}{3.087}\sqrt{2.010} = 0.817$$

(33) From item (12) and figure 3(b)

$$\left(\frac{pA}{m\sqrt{gRT}}\right)_{en} = 2.913$$

(34) From item (30) and figure 3

$$\left(\frac{pA}{m\sqrt{gRT}}\right)_{ex} = 1.420$$

(35) From items (5) and (32)

$$P_{ex} = 0.817 \times 2160 = 1765 \text{ (lb)/(sq ft)}$$

(36) From items (11) and (33)

$$\left(\frac{P}{p}\right)_{en} = \frac{3.087}{2.913} = 1.059$$

so that, from item (5)

$$p_{en} = \frac{2160}{1.059} = 2040 \text{ (lb)/(sq ft)}$$

(37) From items (31) and (34)

$$\left(\frac{P}{p}\right)_{ex} = \frac{1.778}{1.420} = 1.252$$

so that, from item (35)

$$p_{ex} = \frac{1765}{1.252} = 1410 \text{ (lb)/(sq ft)}$$

(38) From items (4) and (9)

$$T_{ex} = 2.010 \times 610 = 1226^{\circ} \text{ R}$$

Example II - Evaluation of $\left(\frac{L}{D_e}\right)_{eff}$

The method of successive approximation must be used in order to obtain consistent values of $\left(\frac{L}{D_e}\right)_{eff}$ and average fluid temperature. The variations of specific heat c_p and absolute viscosity μ of air with temperature, as obtained from reference 8, are presented in figure 6 to aid in this determination.

(39) From figure 6 for $T_w = 2000^{\circ}$ R (item (6))

$$c_{p,w} = 0.2775$$

$$\mu_w = 30.3 \times 10^{-6}$$

(40) Take $T_{av} = 750^{\circ}$ R as a first approximation in which case from figure 6

$$c_{p,av} = 0.2425$$

1004

(41) From equation (21) and items (1), (2), (6), (10), (39), and (40), noting that μ_r equals 12.3×10^{-6} (SYMBOLS)

$$\left(\frac{L}{D_e}\right)_{eff} = \left(\frac{0.022}{0.023}\right)\left(\frac{750}{2000}\right)^{0.8}\left(\frac{0.2775}{0.2425}\right)\left(\frac{30.3\times10^{-6}}{12.3\times10^{-6}}\right)^{0.2}(0.6837\times0.0833)^{-0.2}\left(\frac{7}{0.0833}\right)$$

$$= 89.1 \text{ first approximation}$$

(42) From equation (15) and items (8) and (41)

$$\frac{T_{ex}}{T_{en}} = 1 + (3.279 - 1)\left(1 - e^{-0.00568\times89.1}\right) = 1.9052 \text{ first approximation}$$

(43) From items (4) and (42)

$$T_{av} = T_{en}\left(\frac{1+\frac{T_{ex}}{T_{en}}}{2}\right) = 610\left(\frac{1+1.9052}{2}\right) = 886^\circ \text{ R second approximation}$$

in which case from figure 6, $c_{p,av} = 0.2455$

(44) From equation (21) and items (1), (2), (6), (10), (39), and (43)

$$\left(\frac{L}{D_e}\right)_{eff} = \left(\frac{0.022}{0.023}\right)\left(\frac{886}{2000}\right)^{0.8}\left(\frac{0.2775}{0.2455}\right)\left(\frac{30.3\times10^{-6}}{12.3\times10^{-6}}\right)^{0.2}(0.6837\times0.0833)^{-0.2}\left(\frac{7}{0.0833}\right)$$

$$= 100.6 \text{ second approximation}$$

(45) From equation (15) and items (8) and (44)

$$\frac{T_{ex}}{T_{en}} = 1 + (3.279 - 1)\left(1 - e^{-0.00568 \times 100.6}\right) = 1.993 \text{ second approximation}$$

(46) From items (4) and (45)

$$T_{av} = 610\left(\frac{1 + 1.993}{2}\right) = 913^{\circ} \text{ R third approximation}$$

in which case, $c_{p,av} = 0.2463$

(47) From equation (21) and items (1), (2), (6), (10), (39), and (46)

$$\left(\frac{L}{D_e}\right)_{eff} = \left(\frac{0.022}{0.023}\right)\left(\frac{913}{2000}\right)^{0.8}\left(\frac{0.2775}{0.2463}\right)\left(\frac{30.3 \times 10^{-6}}{12.3 \times 10^{-6}}\right)^{0.2}(0.6837 \times 0.0833)^{-0.2}\left(\frac{7}{0.0833}\right)$$

$$= 102.7 \text{ third approximation}$$

(48) From equation (15) and items (8) and (47)

$$\frac{T_{ex}}{T_{en}} = 1 + (3.279 - 1)\left(1 - e^{-0.00568 \times 102.7}\right) = 2.007 \text{ third approximation}$$

(49) Repetition of the foregoing procedure gives for the fourth approximation

$$T_{av} = 917^{\circ} \text{ R}$$

$$\left(\frac{L}{D_e}\right)_{eff} = 103.0$$

$$\frac{T_{ex}}{T_{en}} = 2.010$$

which are practically identical with the third approximation values.

The values of T_{av}, $\left(\frac{L}{D_e}\right)_{eff}$, and $\frac{T_{ex}}{T_{en}}$ given in item (49) represent the convergent values. It is evident that the third approximation values could have been taken as the convergent values with negligible error; in general, the third approximation values are sufficiently accurate.

Example III - Determination of Exit End Losses

Assume that the flow at the exit of the tube of example I suddenly discharged into a duct having twice the cross-sectional area of the tube (in which case, $f = 0.50$).

Determine:

(a) Static and total pressures at the duct cross section where uniform flow is reestablished (referred to as station d in fig. 4).

(b) Drop in static and total pressures from entrance of tube of example I to duct cross section where uniform flow is reestablished (in fig. 4, from station en to station d).

(1) From the results of example I (items (30), (31), and (34)), the flow parameters at the tube exit are:

$$\left(\frac{mV+pA}{m\sqrt{gRT}}\right)_{ex} = 2.080$$

$$\left(\frac{PA}{m\sqrt{gRT}}\right)_{ex} = 1.778$$

$$\left(\frac{pA}{m\sqrt{gRT}}\right)_{ex} = 1.420$$

(2) From equation (24) and item (1) of this example for $f = 0.50$, noting that in figure 4 the small area is at station ex and the large area at station d

$$\left(\frac{mV+pA}{m\sqrt{gRT}}\right)_d = 2.080 + 1.420\left(\frac{1}{0.50} - 1\right) = 3.500$$

(3) From item (2) and figures 2 and 3

$$\left(\frac{PA}{m\sqrt{gRT}}\right)_d = 3.348$$

$$\left(\frac{pA}{m\sqrt{gRT}}\right)_d = 3.189$$

(4) From items (1) and (3) noting that $\frac{A_{ex}}{A_d} = f = 0.50$ and that m and T are constant across the enlargement

$$\frac{P_d}{P_{ex}} = \left(\frac{PA}{m\sqrt{gRT}}\right)_d \left(\frac{m\sqrt{gRT}}{PA}\right)_{ex} \frac{A_{ex}}{A_d} = \frac{3.348}{1.778} \times 0.50 = 0.942$$

$$\frac{p_d}{p_{ex}} = \left(\frac{pA}{m\sqrt{gRT}}\right)_d \left(\frac{m\sqrt{gRT}}{pA}\right)_{ex} \frac{A_{ex}}{A_d} = \frac{3.189}{1.420} \times 0.50 = 1.123$$

(5) From example I, $P_{ex} = 1765$ pounds per square foot and $p_{ex} = 1410$ pounds per square foot, which from item (4) gives

$$P_d = 0.942 \times 1765 = 1663 \text{ (lb)/(sq ft)}$$

$$p_d = 1.123 \times 1410 = 1583 \text{ (lb)/(sq ft)}$$

(6) The drop in total pressure from station en to station d in figure 4 is, from item (5) of example I and from item (5) of this example,

$$\Delta P_{en-d} = 2160 - 1663 = 497 \text{ (lb)/(sq ft)}$$

If the flow process at the tube entrance were isentropic, the value of total-pressure drop given by item (6) would also be obtained across the entire tube, including all end losses.

(7) The drop in static pressure from station en to station d in figure 4 is, from item (36) of example I and from item (5) of this example,

$$\Delta p_{en-d} = 2040 - 1583 = 457 \text{ (lb)/(sq ft)}$$

The static-pressure drop obtained at the tube entrance for an isentropic flow process can be calculated by standard equations and added to the value of pressure drop given by item (7) to obtain the over-all static-pressure drop across the tube, including all end losses.

Lewis Flight Propulsion Laboratory,
National Advisory Committee for Aeronautics,
Cleveland, Ohio.

REFERENCES

1. Nielsen, Jack N.: High-Altitude Cooling. III - Radiators. NACA ARR No. L4I11b, 1944.

2. Becker, John V., and Baals, Donald D.: Simple Curves for Determining the Effects of Compressibility on Pressure Drop through Radiators. NACA ACR No. L4I23, 1944.

3. Habel, Louis W., and Gallagher, James J.: Tests to Determine the Effect of Heat on the Pressure Drop through Radiator Tubes. NACA TN No. 1362, 1947.

4. Shapiro, Ascher H., and Hawthorne, W. R.: The Mechanics and Thermodynamics of Steady One-Dimensional Gas Flow. Jour. Appl. Mech., vol. 14, no. 4, Dec. 1947, pp. A317-A336.

5. Turner, L. Richard, Addie, Albert N., and Zimmerman, Richard H.: Charts for the Analysis of One-Dimensional Steady Compressible Flow. NACA TN No. 1419, 1948.

6. Humble, Leroy V., Lowdermilk, Warren H., and Grele, Milton: Heat Transfer from High Temperature Surfaces to Fluids. I - Preliminary Investigation with Air in Inconel Tube with Rounded Entrance, Inside Diameter of 0.4 Inch and Length of 24 Inches. NACA RM No. E7L31, 1948.

7. McAdams, William H.: Heat Transmission. McGraw-Hill Book Co., Inc., 2d ed., 1942.

8. Tribus, Myron, and Boelter, L. M. K.: An Investigation of Aircraft Heaters. II - Properties of Gases. NACA ARR, Oct. 1942.

TABLE I - COMPARISON OF CALCULATED AND MEASURED[a] RESULTS

Average T_w (°R)	Entrance conditions				Exit	Measured results				Calculated results				Percentage difference in	
	Reynolds number	P (lb/sq ft)	T (°R)	M	M	$\frac{p_{ex}}{p_{en}}$	$\frac{T_{ex}}{T_{en}}$	Δp (lb/sq ft)	ΔT (°R)	$\frac{p_{ex}}{p_{en}}$	$\frac{T_{ex}}{T_{en}}$	Δp (lb/sq ft)	ΔT (°R)	Δp (lb/sq ft)	ΔT (°R)
1672	184,000	4527	528	0.37	0.84	0.551	1.710	2031	375	0.544	1.699	2065	369	1.7	-1.6
1072	155,000	3682	554	.41	.70	.639	1.359	1329	199	.657	1.348	1264	185	-4.9	-3.0
861	219,000	4458	540	.46	.87	.568	1.218	1926	118	.553	1.218	1993	118	3.5	0
1670	263,000	6186	530	.39	1.00 choke	.464	1.651	3315	345	.458	1.645	3353	342	[b]1.2	-1.0
1752	53,600	2417	527	.21	.32	.881	1.967	288	510	.889	1.939	267	495	-7.1	-3.0

[a]Data from reference 6.

[b]Calculated choking length less than actual choking length by 2.6 percent.

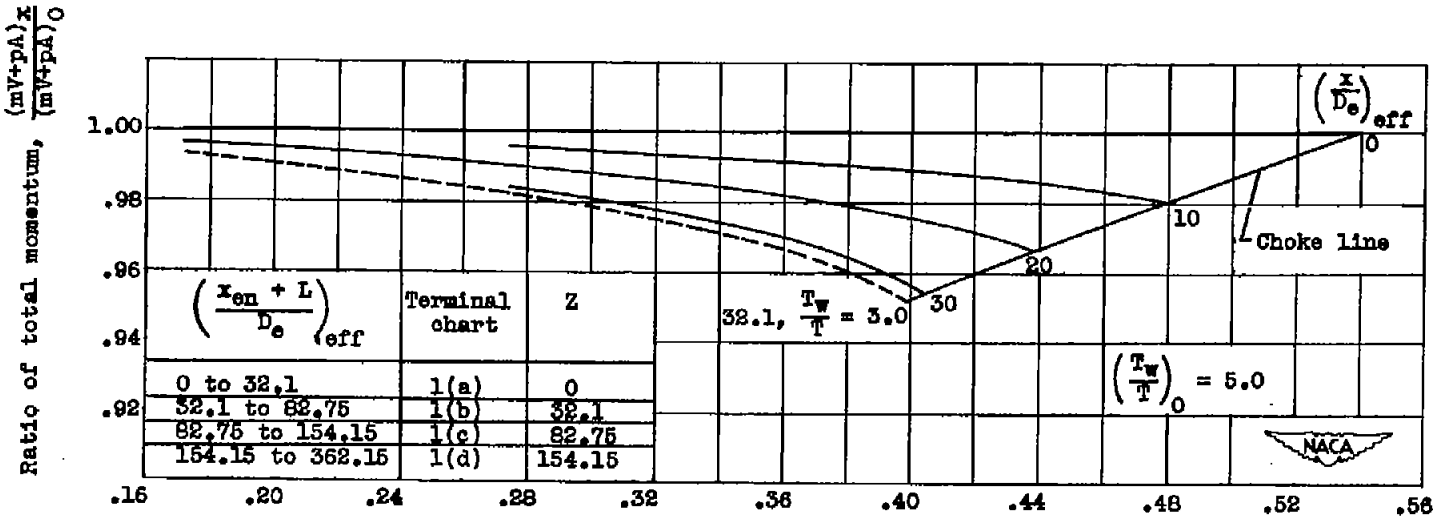

Reciprocal of total-momentum parameter at reference station, $\left(\frac{m\sqrt{gRT}}{mV+pA}\right)_0$

(a) Reference station characterized by $\left(\frac{T_w}{T}\right)_0$ = 5.0.

Figure 1. - Variation of total momentum with distance $\left(\frac{x}{D_e}\right)_{eff}$ as a function of the total-momentum parameter at the reference station. Turbulent flow, air (γ = 1.400), heat addition at constant wall temperature. (A 7 - by 22-inch print of this figure is attached.)

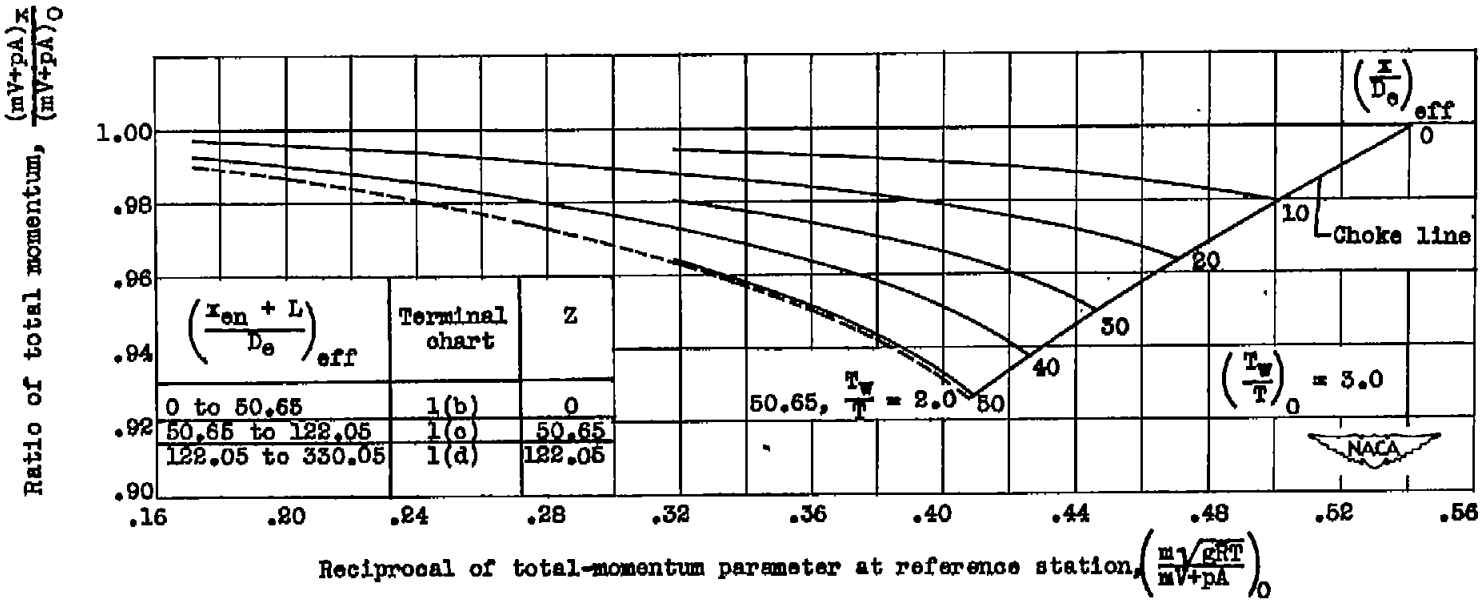

(b) Reference station characterized by $\left(\frac{T_w}{T}\right)_0 = 3.0$.

Figure 1. - Continued. Variation of total momentum with distance $\left(\frac{x}{D_e}\right)_{eff}$ as a function of the total-momentum parameter at the reference station. Turbulent flow, air (γ = 1.400), heat addition at constant wall temperature. (A 9- by 22-inch print of this figure is attached.)

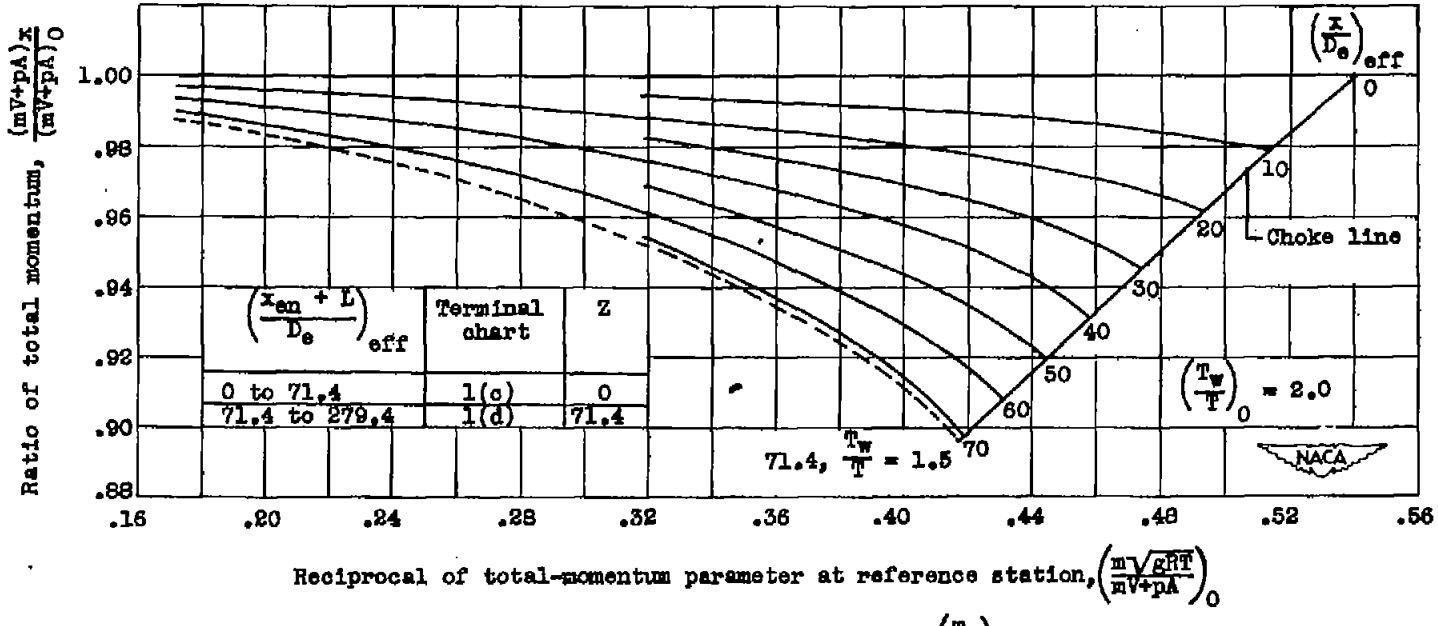

(c) Reference station characterized by $\left(\frac{T_w}{T}\right)_0 = 2.0$.

Figure 1. - Continued. Variation of total momentum with distance $\left(\frac{x}{D_e}\right)_{eff}$ as a function of the total-momentum parameter at the reference station. Turbulent flow, air ($\gamma = 1.400$), heat addition at constant wall temperature. (A 10- by 22-inch print of this figure is attached.)

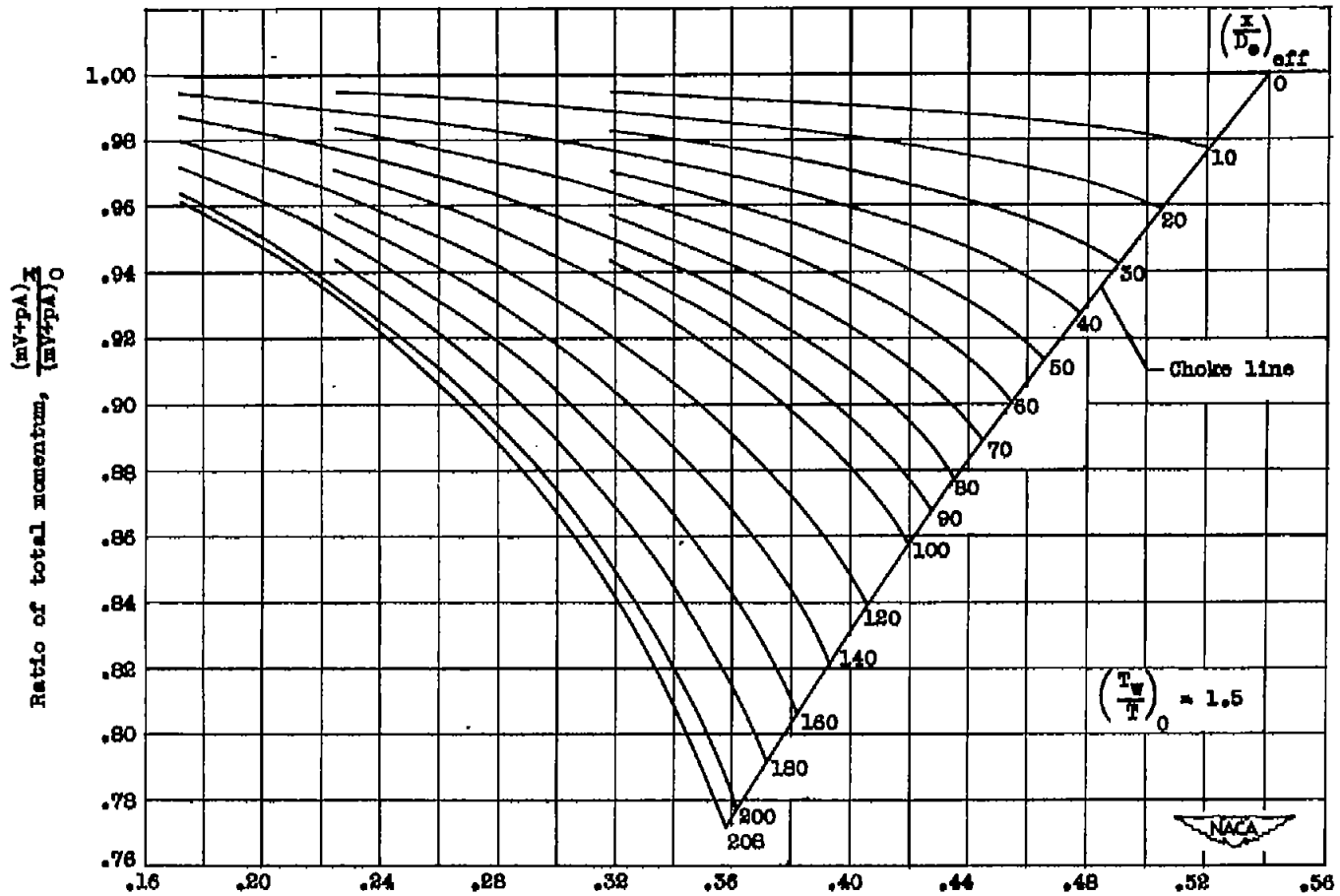

(d) Reference station characterized by $\left(\frac{T_w}{T}\right)_0 = 1.5$.

Figure 1. - Concluded. Variation of total momentum with distance $\left(\frac{x}{D_e}\right)_{eff}$ as a function of the total-momentum parameter at the reference station. Turbulent flow, air ($\gamma = 1.400$), heat addition at constant wall temperature. (A 16- by 22-inch print of this figure is attached.)

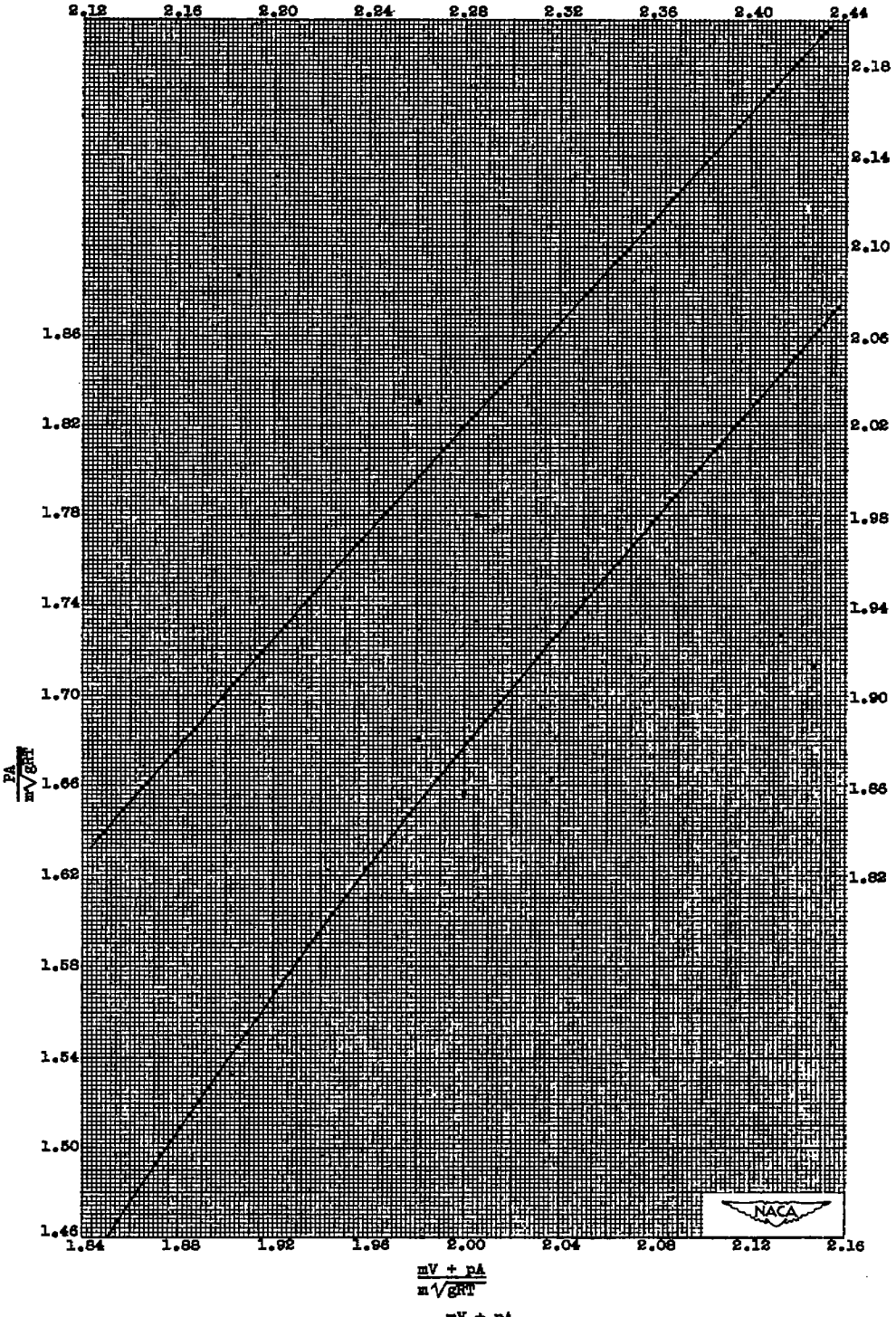

(a) Range of $\frac{mV + pA}{m\sqrt{gRT}}$, 1.852 to 2.42.

Figure 2. - Relation between total-pressure parameter and total-momentum parameter for air ($\gamma = 1.400$).

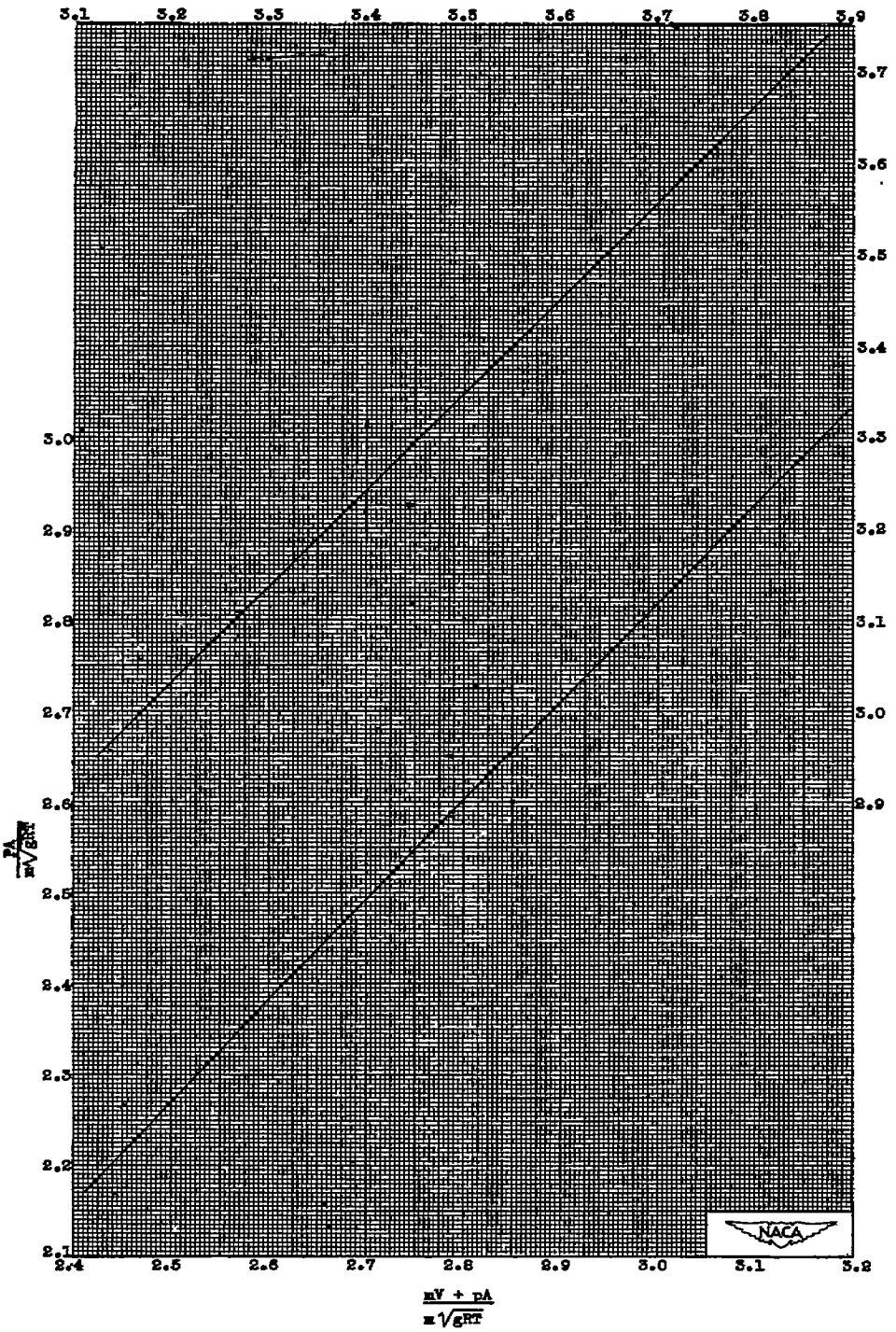

(b) Range of $\frac{\dot{m}V + pA}{\dot{m}\sqrt{gRT}}$, 2.40 to 3.85.

Figure 2. - Continued. Relation between total-pressure parameter and total-momentum parameter for air ($\gamma = 1.400$).

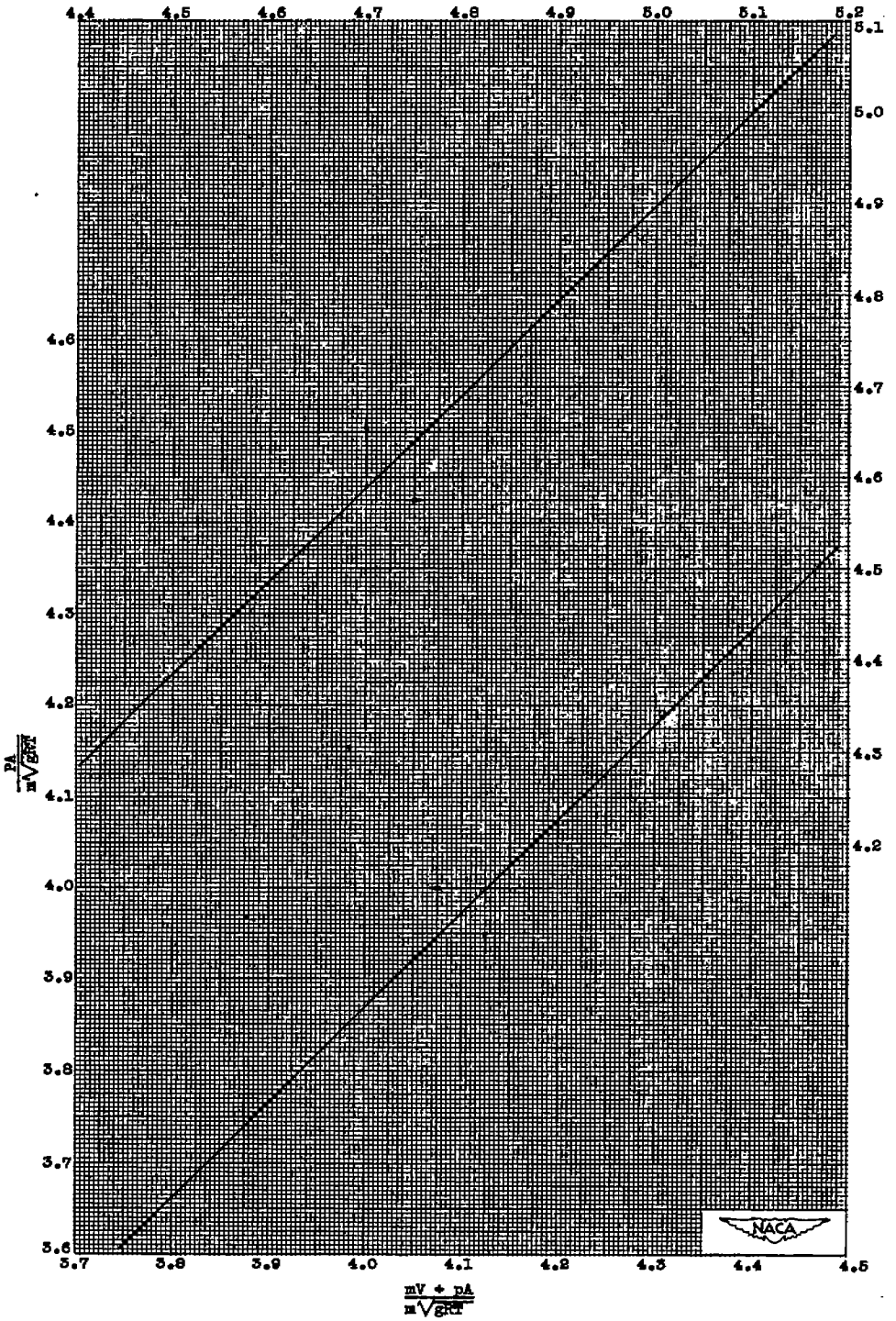

(c) Range of $\frac{mV + pA}{m\sqrt{gRT}}$, 3.75 to 5.15.

Figure 8. - Continued. Relation between total-pressure parameter and total-momentum parameter for air ($\gamma = 1.400$).

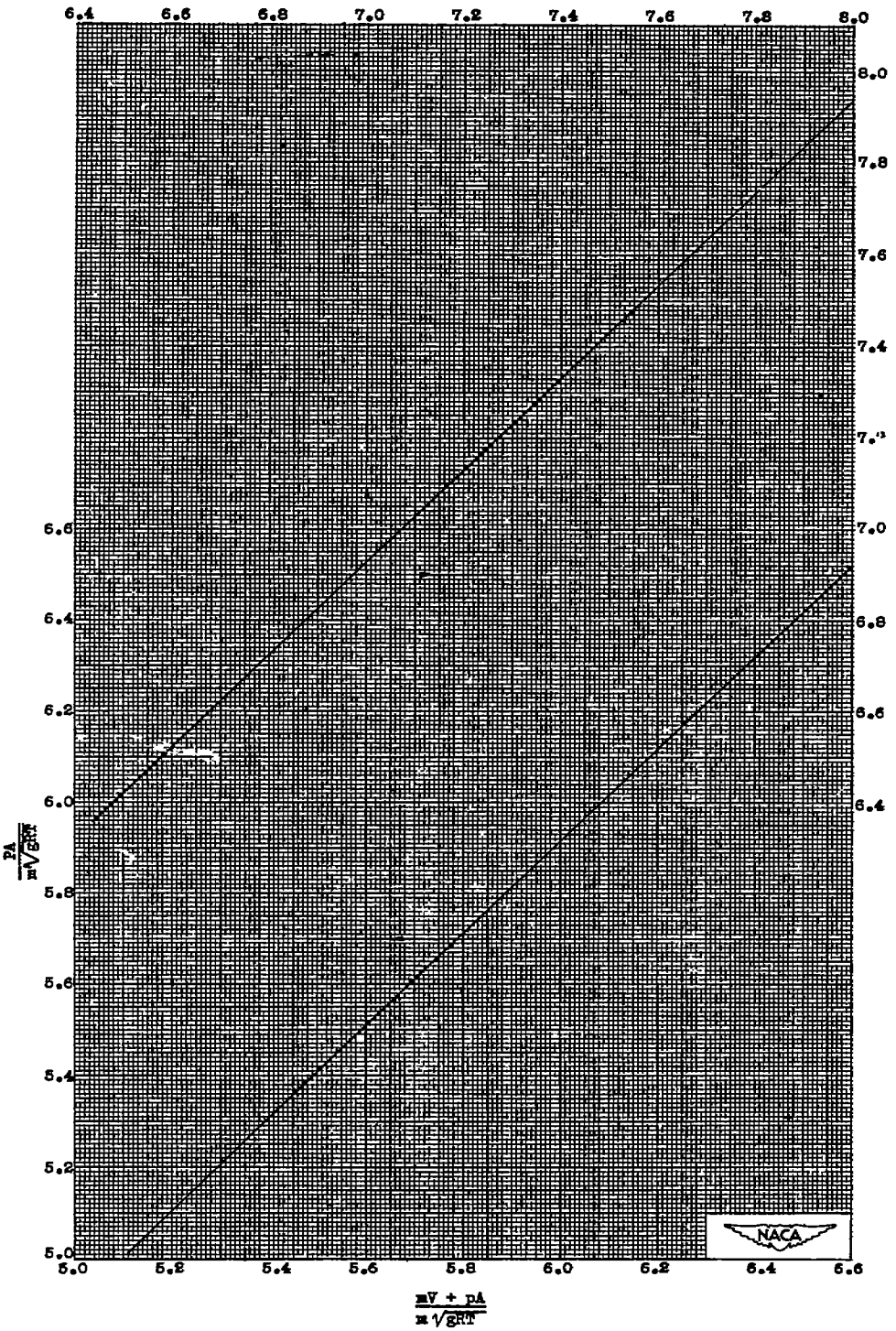

(d) Range of $\frac{mV + pA}{m\sqrt{gRT}}$, 5.15 to 8.00.

Figure 2. - Concluded. Relation between total-pressure parameter and total-momentum parameter for air ($\gamma = 1.400$).

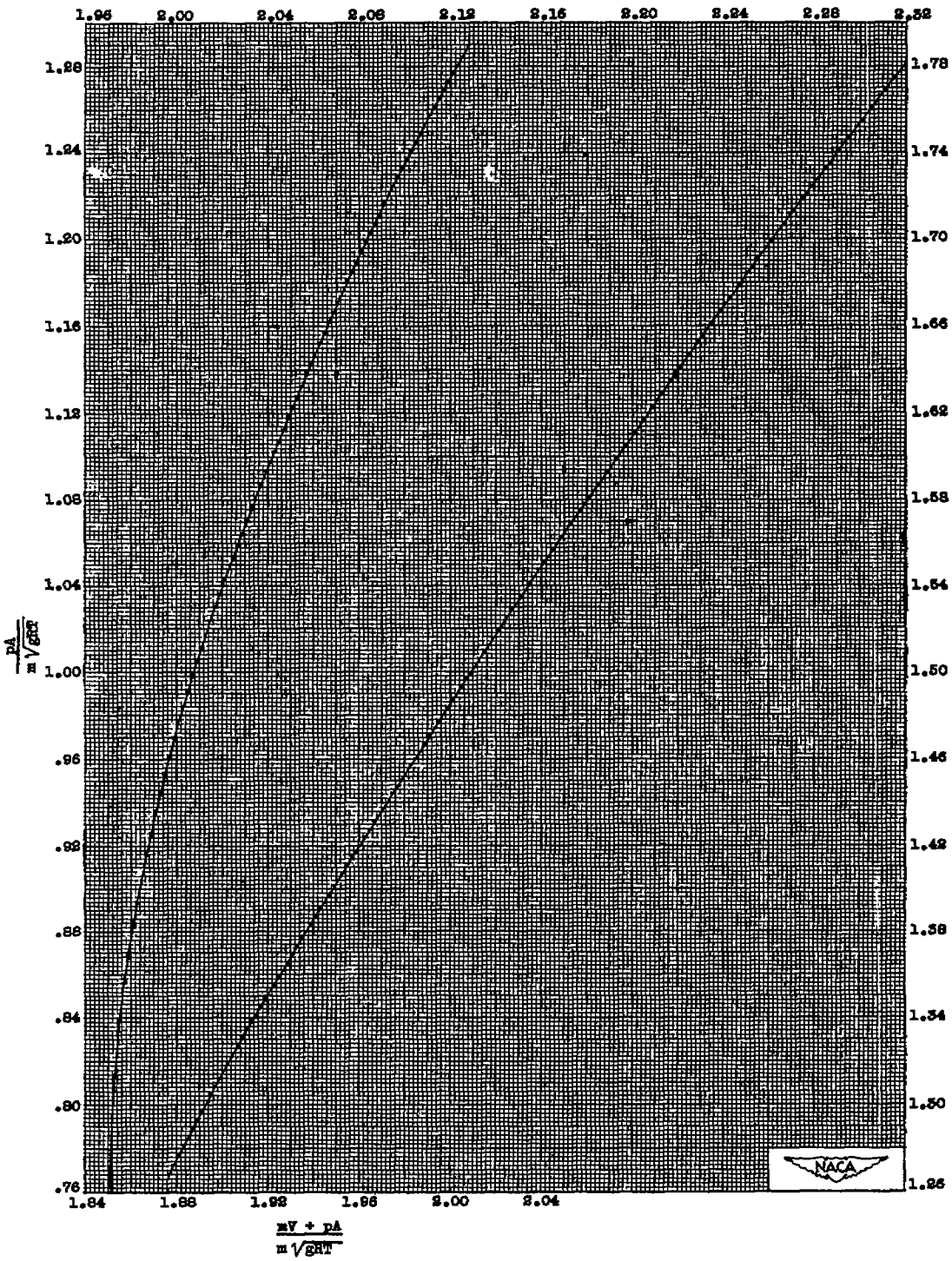

(a) Range of $\frac{mV + pA}{m\sqrt{gRT}}$, 1.852 to 2.32.

Figure 3. - Relation between static-pressure parameter and total-momentum parameter for air (γ = 1.400).

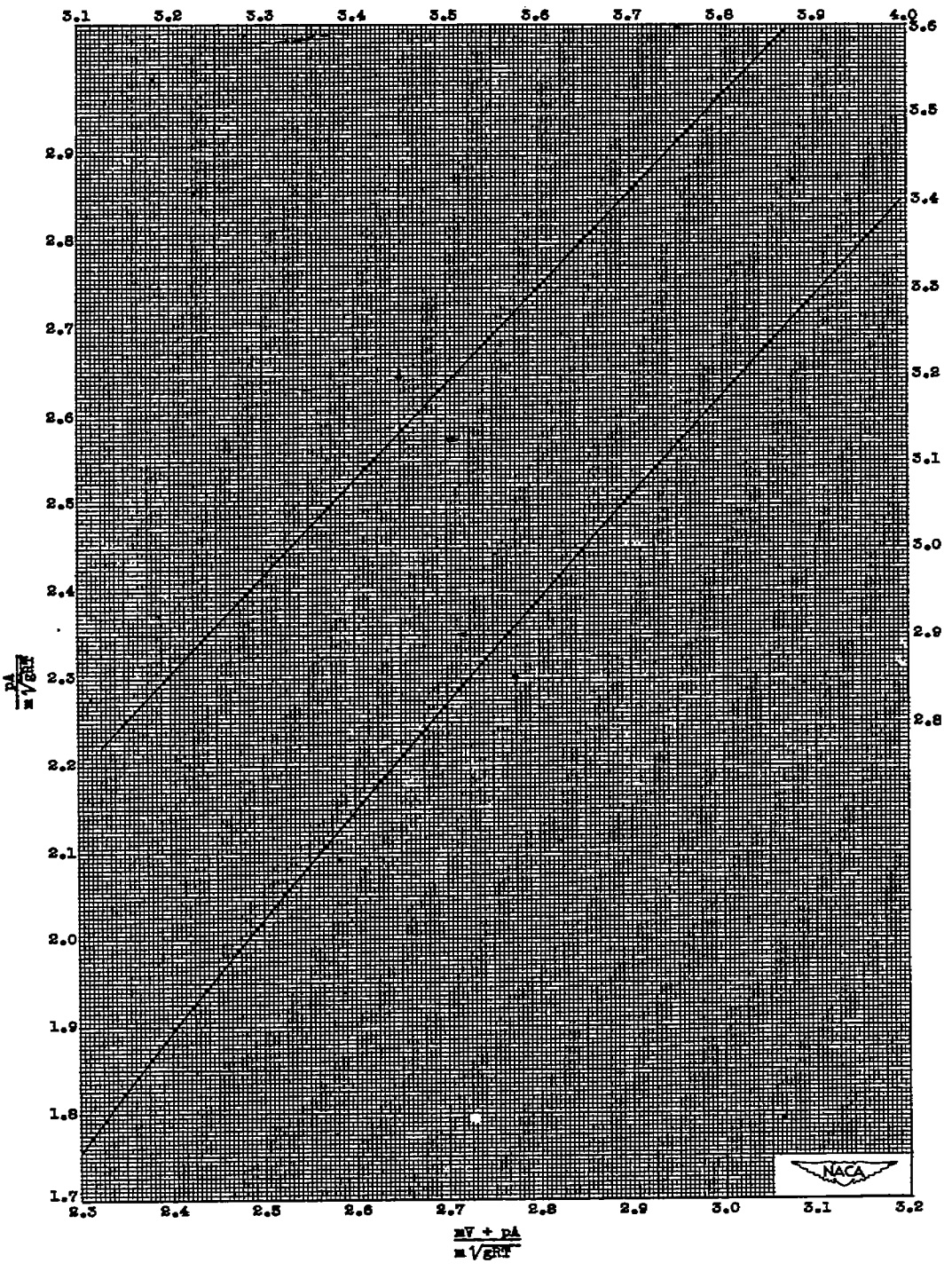

(b) Range of $\frac{wV + pA}{w\sqrt{gRT}}$, 2.30 to 3.85.

Figure 3. - Continued. Relation between static-pressure parameter and total-momentum parameter for air ($\gamma = 1.400$).

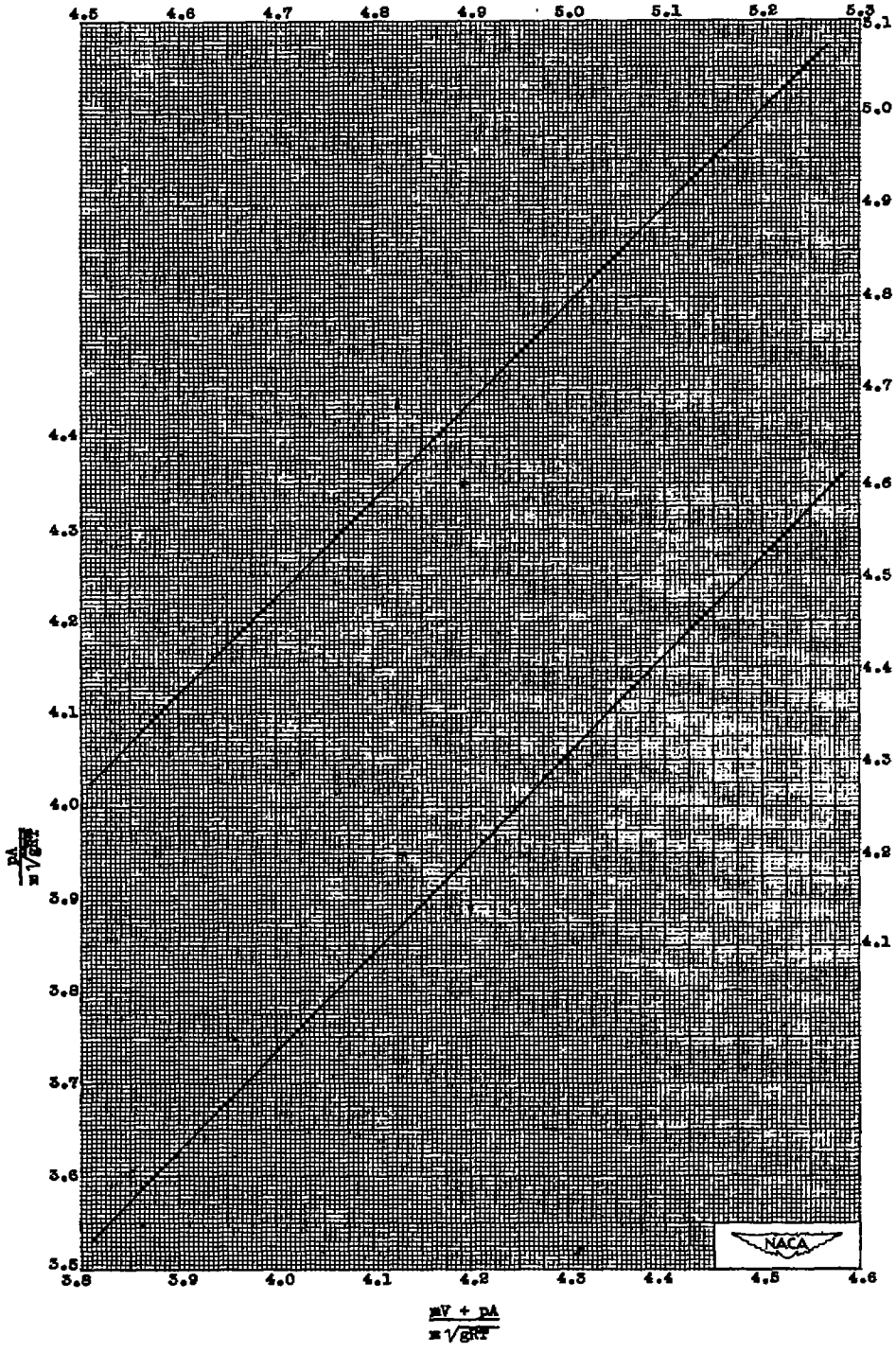

(c) Range of $\frac{wV + pA}{w\sqrt{gRT}}$, 3.80 to 5.25.

Figure 3. - Continued. Relation between static-pressure parameter and total-momentum parameter for air ($\gamma = 1.400$).

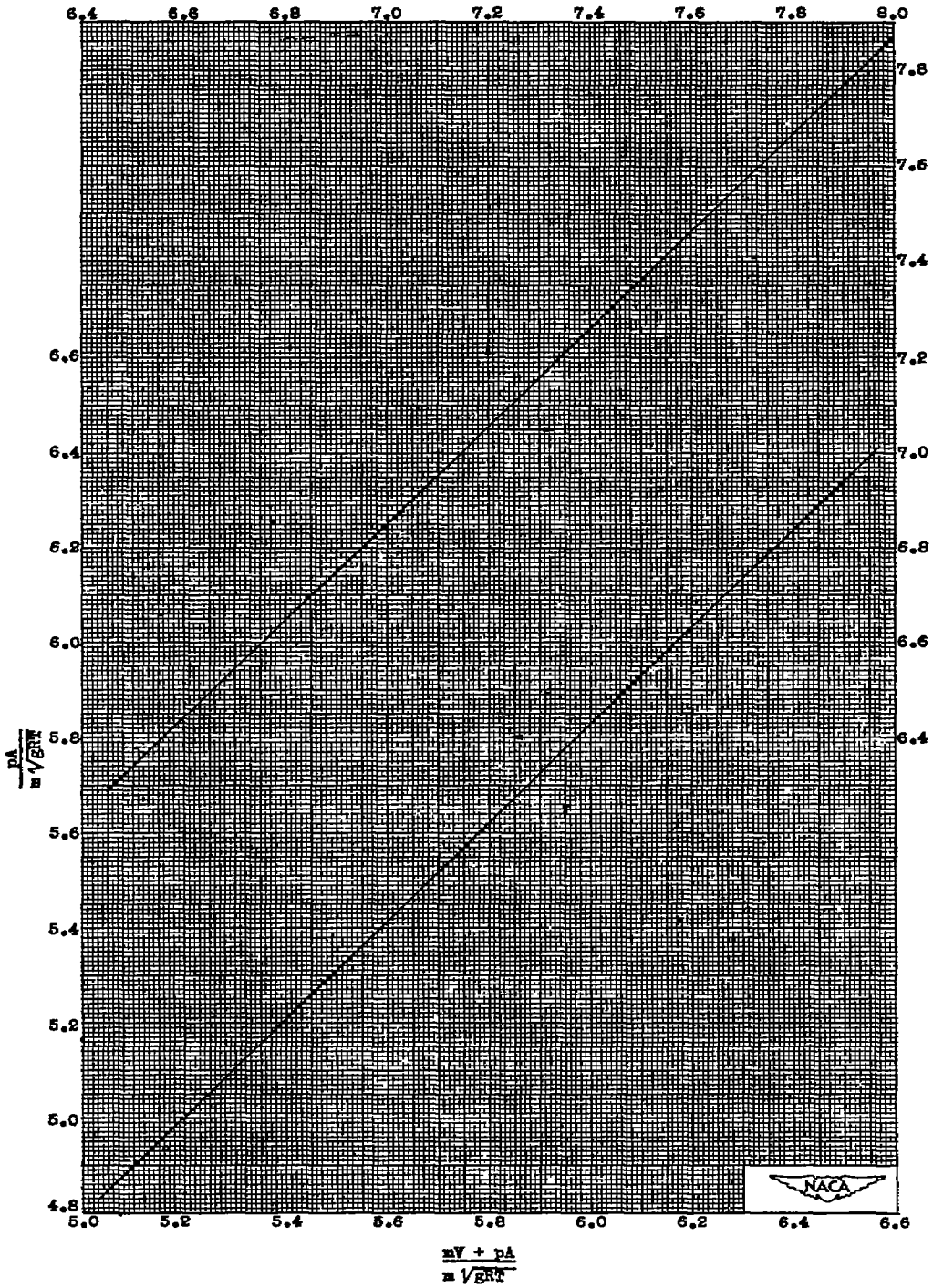

(d) Range of $\frac{mV + pA}{\dot{m}\sqrt{gRT}}$, 5.00 to 8.00.

Figure 3. - Concluded. Relation between static-pressure parameter and total-momentum parameter for air (γ = 1.400).

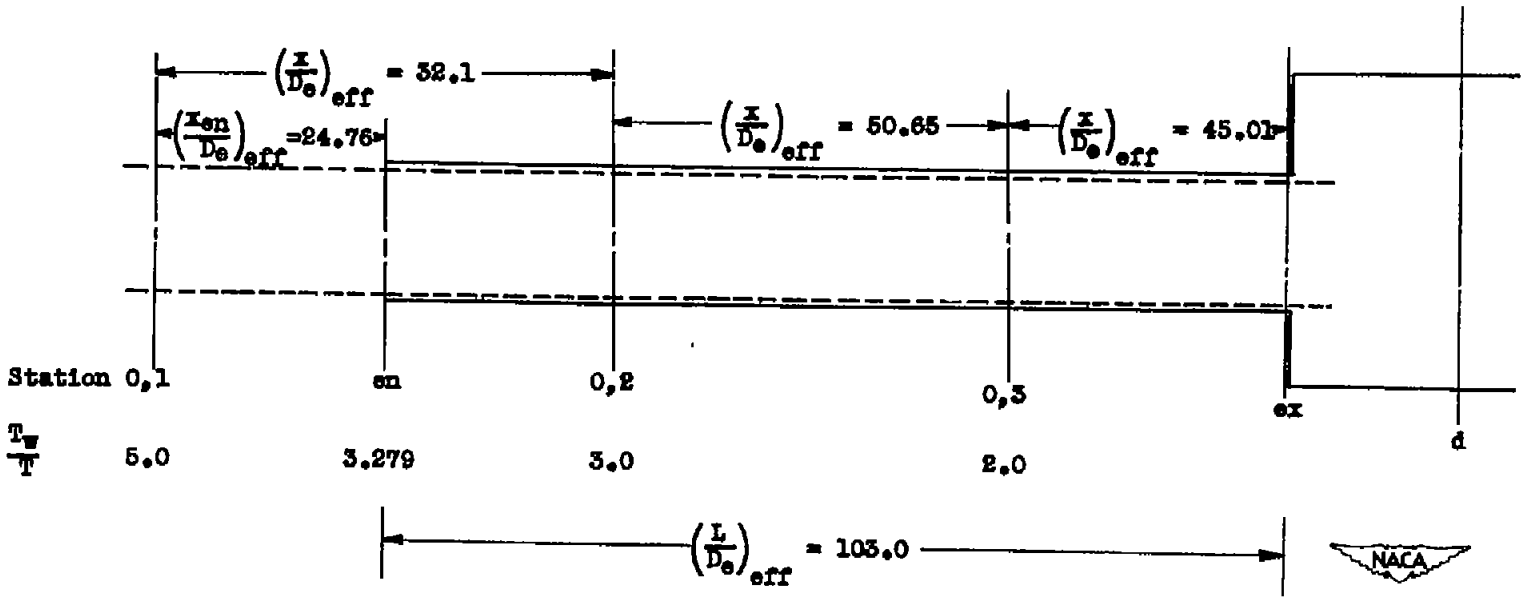

Figure 4. - Schematic diagram of flow passage of examples I, II, and III showing relative positions of various stations in given flow system.

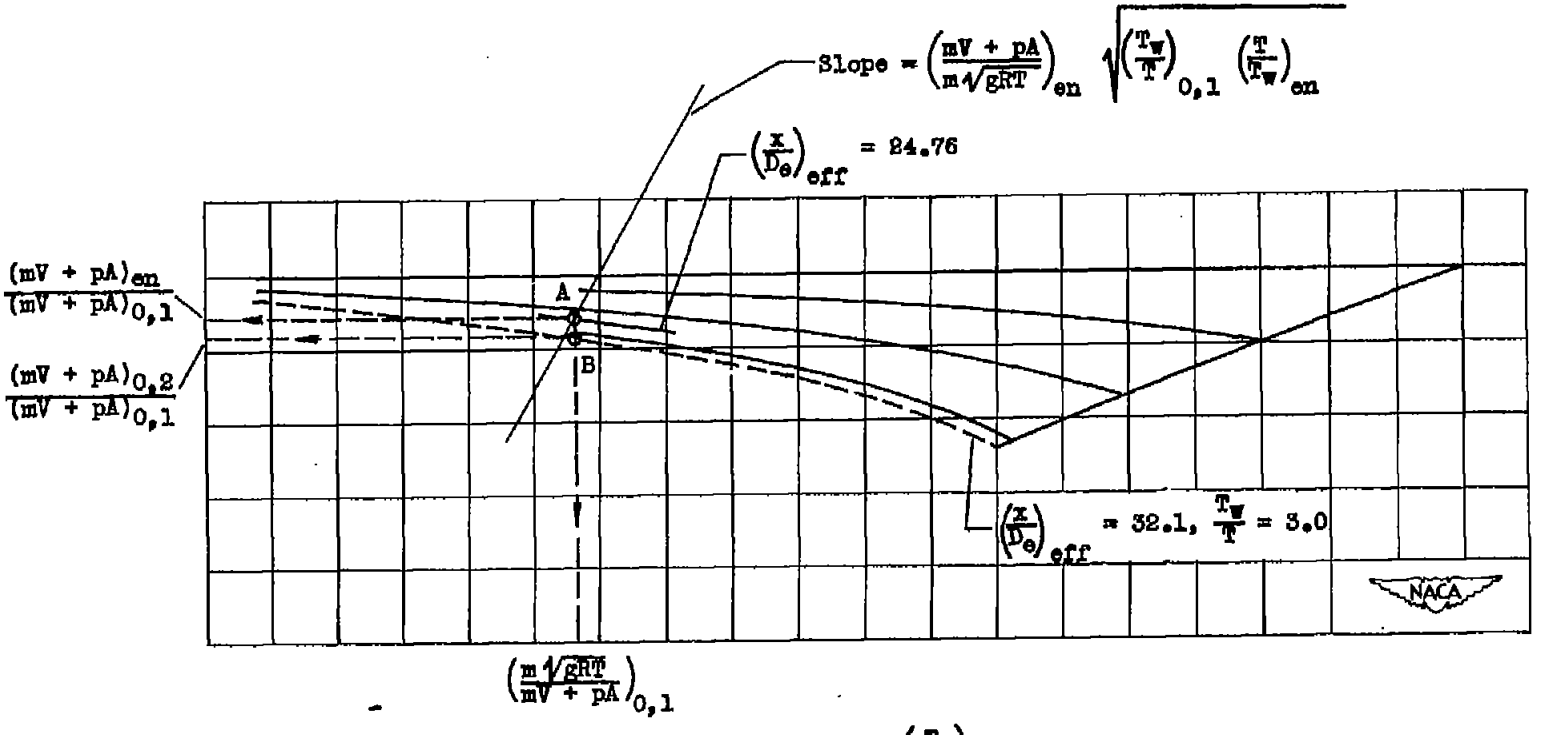

(a) Figure 1(a), $\left(\frac{T_w}{T}\right)_0 = 5.0$.

Figure 5. - Use of figure 1 in solution of problem of example I.

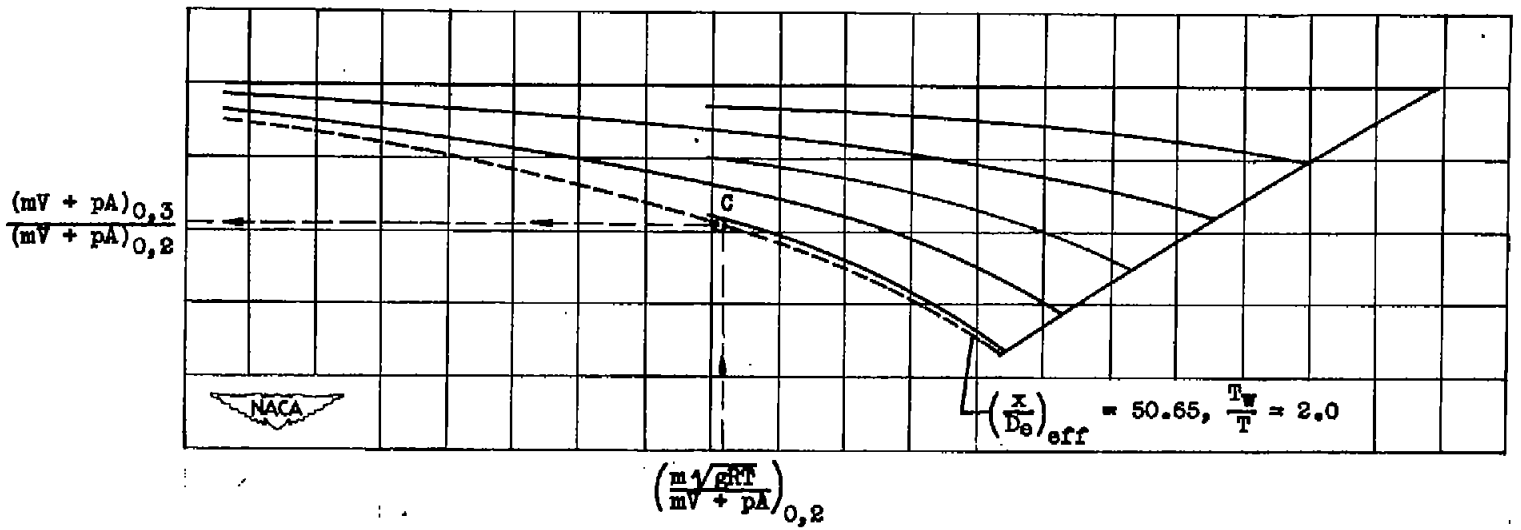

(b) Figure 1(b), $\left(\frac{T_w}{T}\right)_0$ = 3.0.

Figure 5. - Continued. Use of figure 1 in solution of problem of example I.

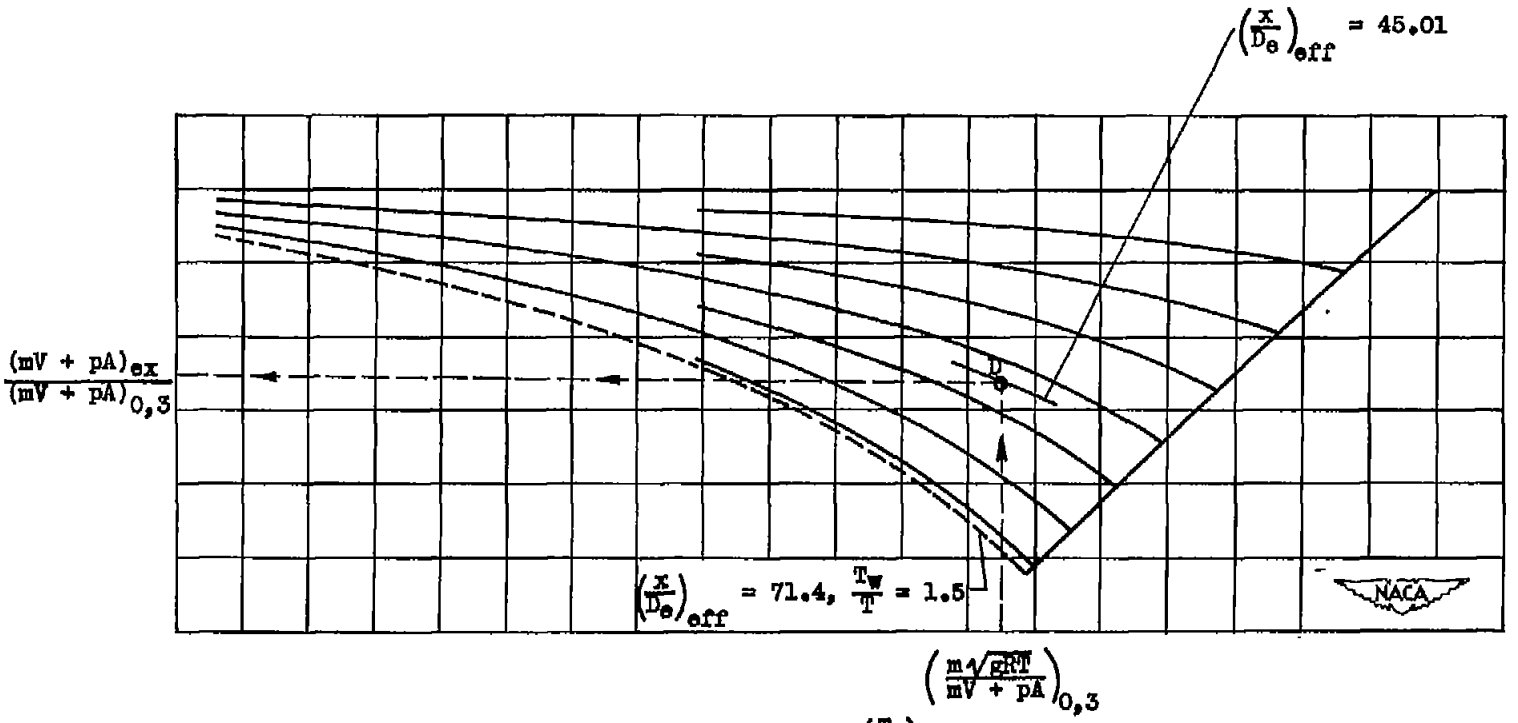

(c) Figure 1(c), $\left(\frac{T_w}{T}\right)_0$ = 2.0.

Figure 5. - Concluded. Use of figure 1 in solution of problem of example I.

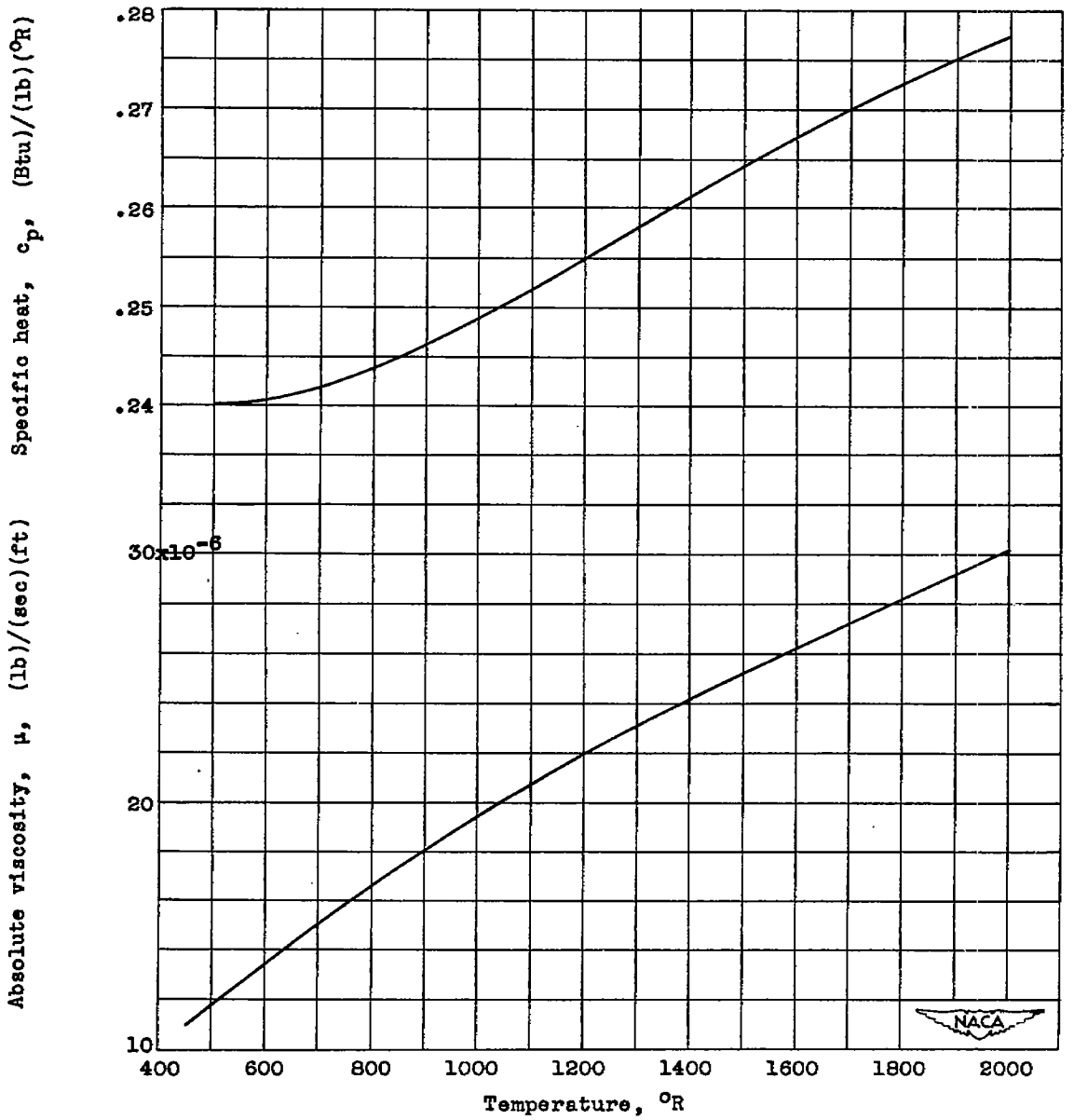

Figure 6. - Variation of absolute viscosity μ and specific heat c_p of air with temperature.

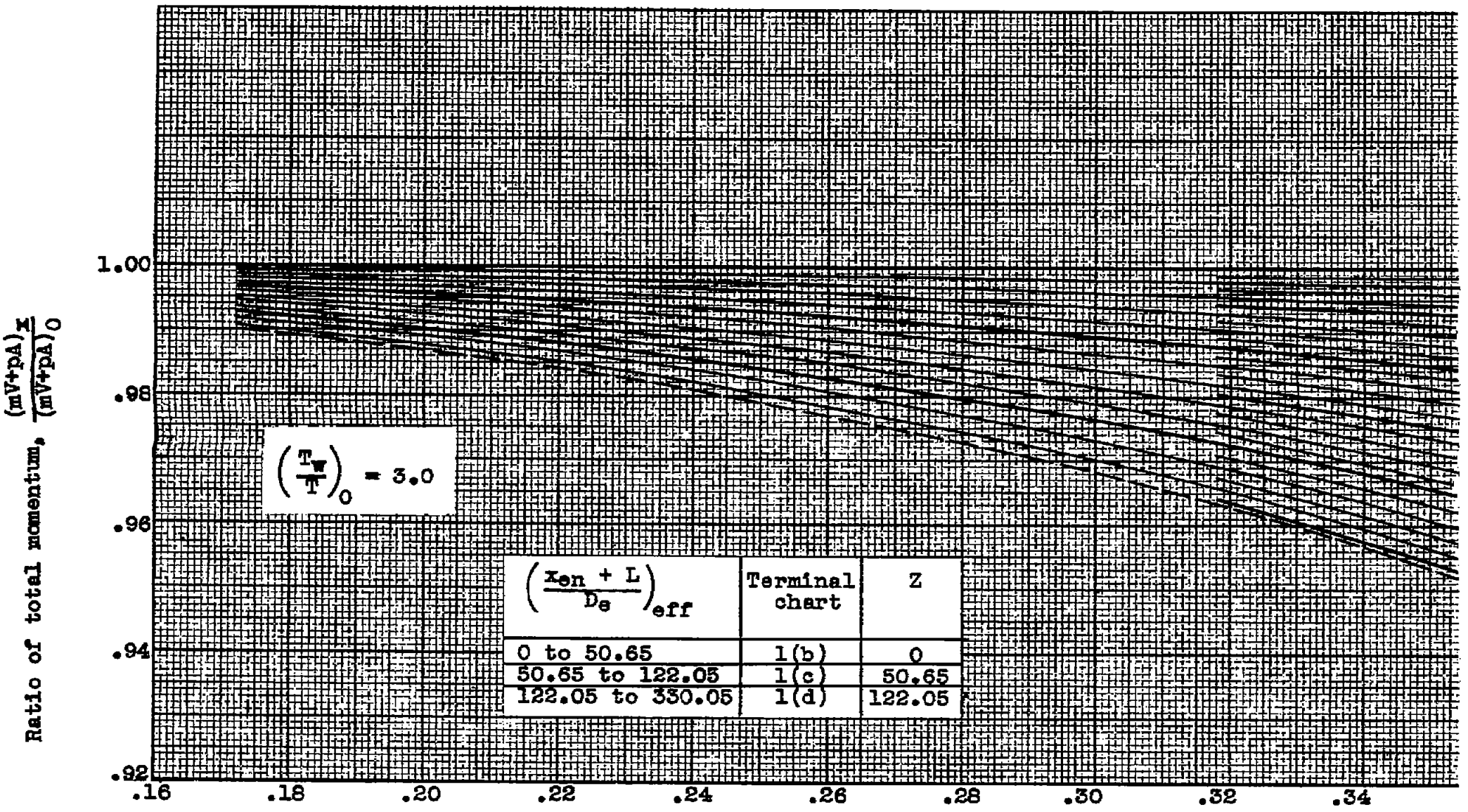

$\left(\frac{x_{en} + L}{D_e}\right)_{eff}$	Terminal chart	Z
0 to 50.65	1(b)	0
50.65 to 122.05	1(c)	50.65
122.05 to 330.05	1(d)	122.05

(b) Reference station char

Figure 1. - Continued. Variation of total momentum with distance $\left(\frac{x}{D_e}\right)_{eff}$ as a function of the tota

heat addition at constant wall t

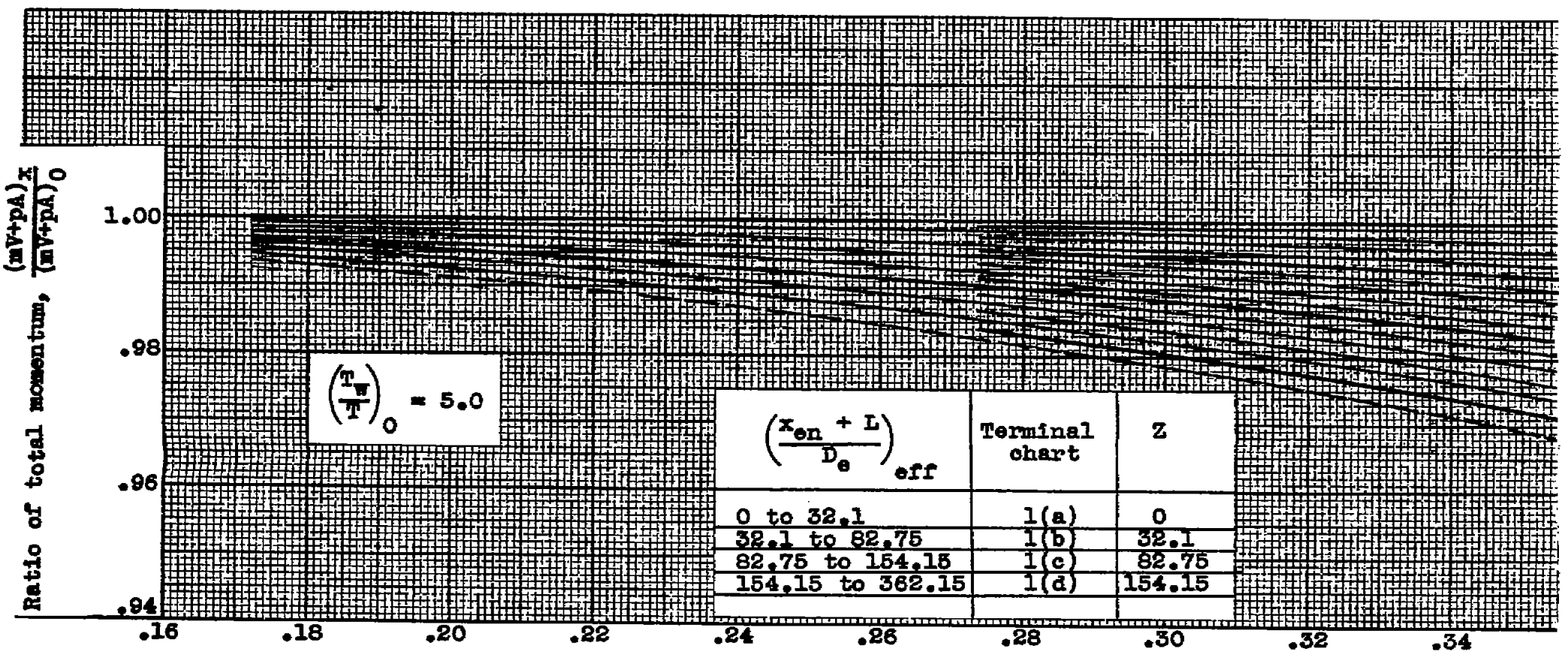

$\left(\frac{x_{en} + L}{D_e}\right)_{eff}$	Terminal chart	Z
0 to 32.1	1(a)	0
32.1 to 82.75	1(b)	32.1
82.75 to 154.15	1(c)	82.75
154.15 to 362.15	1(d)	154.15

(a) Reference station char

Figure 1. - Variation of total momentum with distance $\left(\frac{x}{D_e}\right)_{eff}$ as a function of the total-momentu

constant wall ter

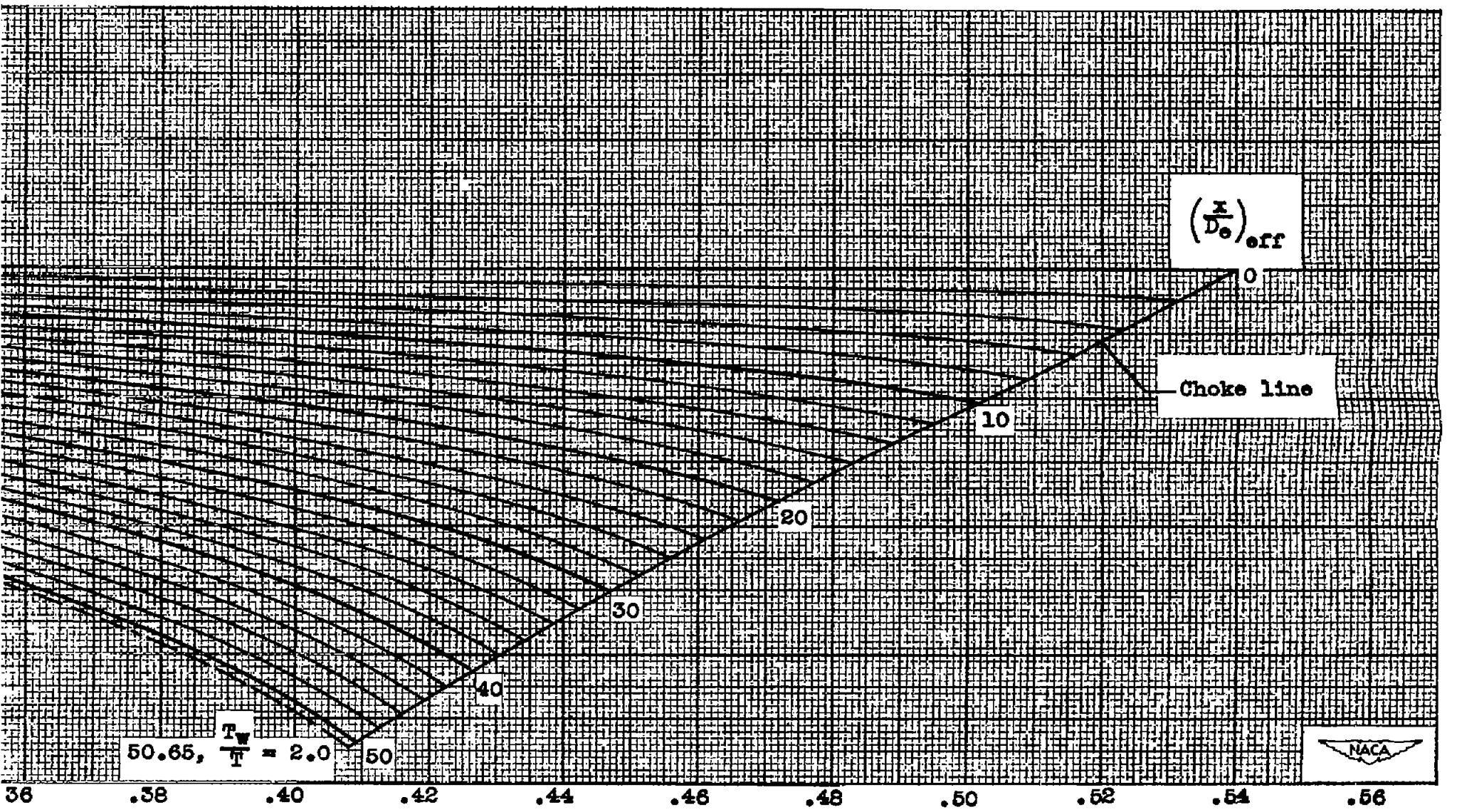

er at reference station, $\left(\frac{m\sqrt{gRT}}{mV+pA}\right)_0$

terized by $\left(\frac{T_w}{T}\right)_0$ = 3.0.

-momentum parameter at the reference station. Turbulent flow, air (γ = 1.400),

mperature.

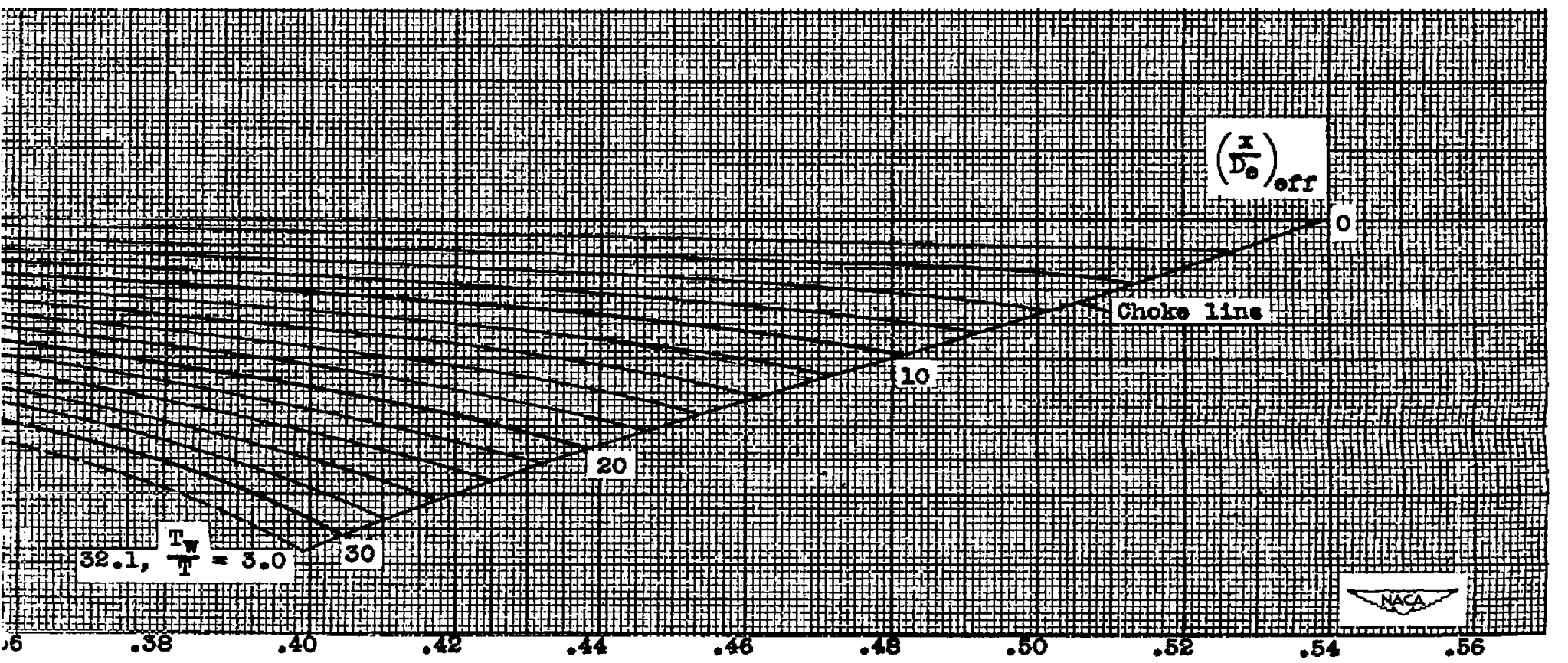

er at reference station, $\left(\frac{m\sqrt{gRT}}{mV+pA}\right)_0$

terized by $\left(\frac{T_w}{T}\right)_0$ = 5.0.

parameter at the reference station. Turbulent flow, air (γ = 1.400), heat addition at

erature.

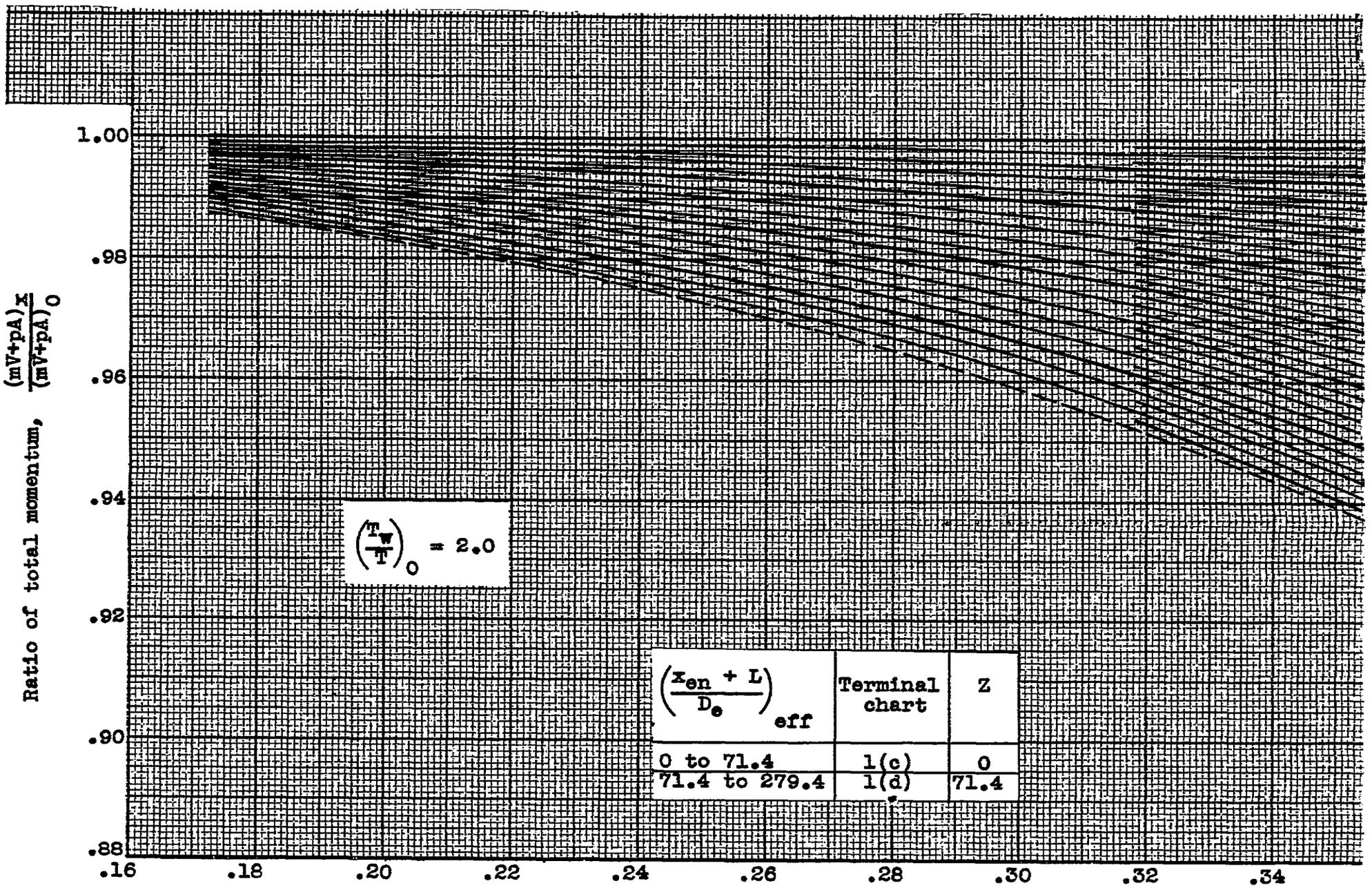

(c) Reference station chara

Figure 1. - Continued. Variation of total momentum with distance $\left(\frac{x}{D_e}\right)_{eff}$ as a function of the tc heat addition at constant wall

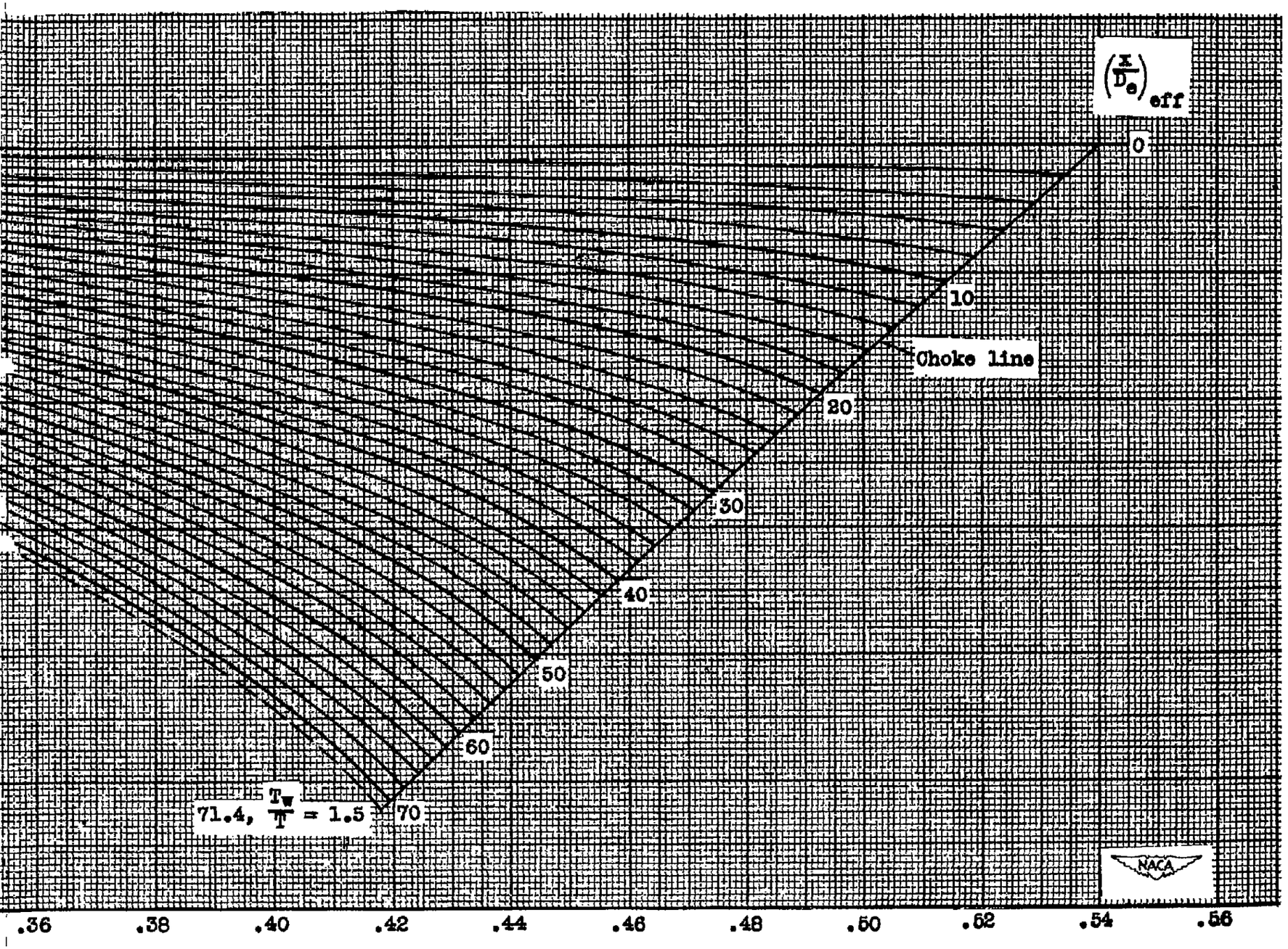

ter at reference station, $\left(\frac{m\sqrt{gRT}}{mV+pA}\right)_0$

acterized by $\left(\frac{T_w}{T}\right)_0 = 2.0$.

tal-momentum parameter at the reference station. Turbulent flow, air ($\gamma = 1.400$),

temperature.

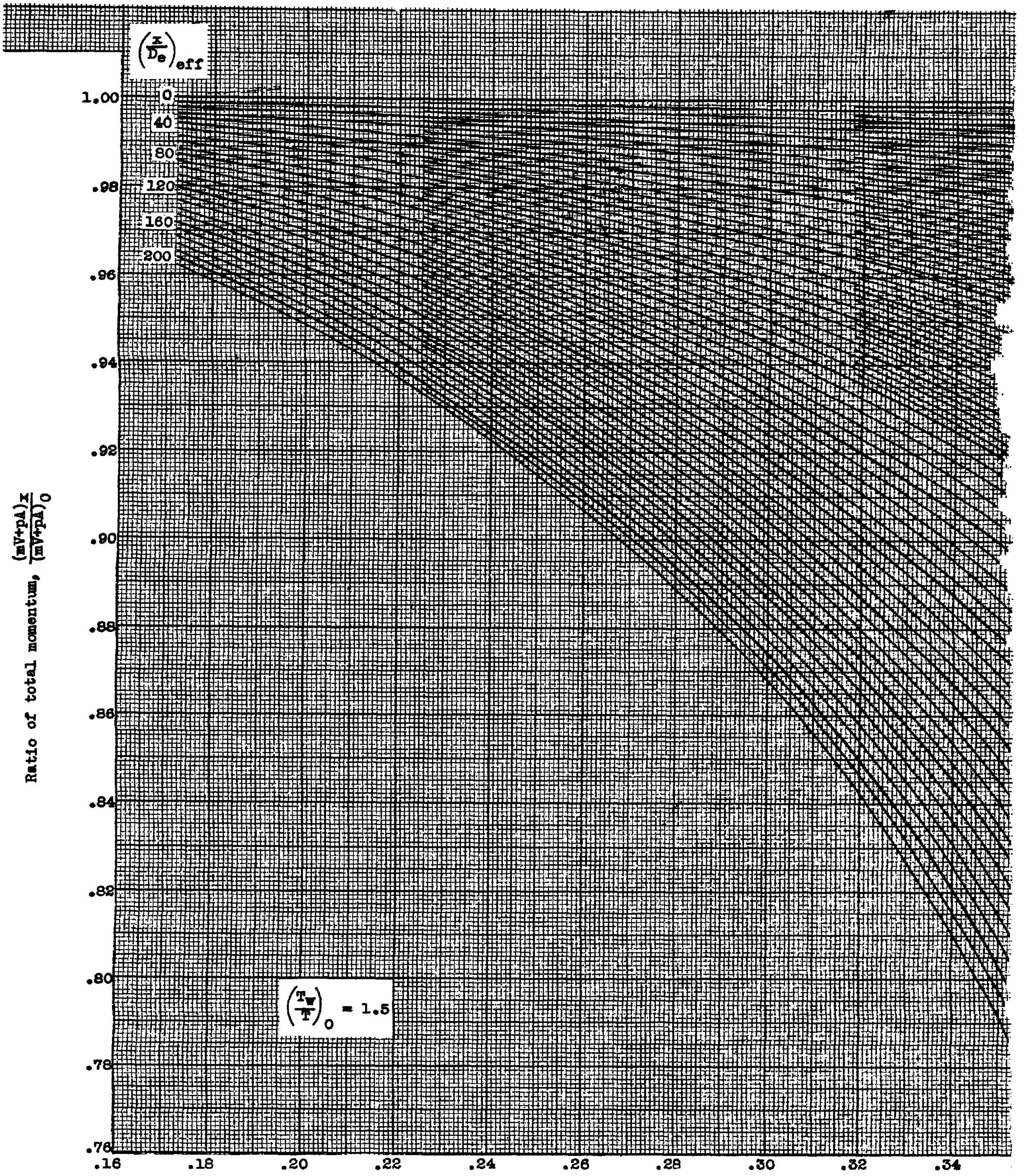

(d) Reference station char

Figure 1. - Concluded. Variation of total momentum with distance $\left(\frac{x}{D_e}\right)_{eff}$ as a function of the t
heat addition at constant wall

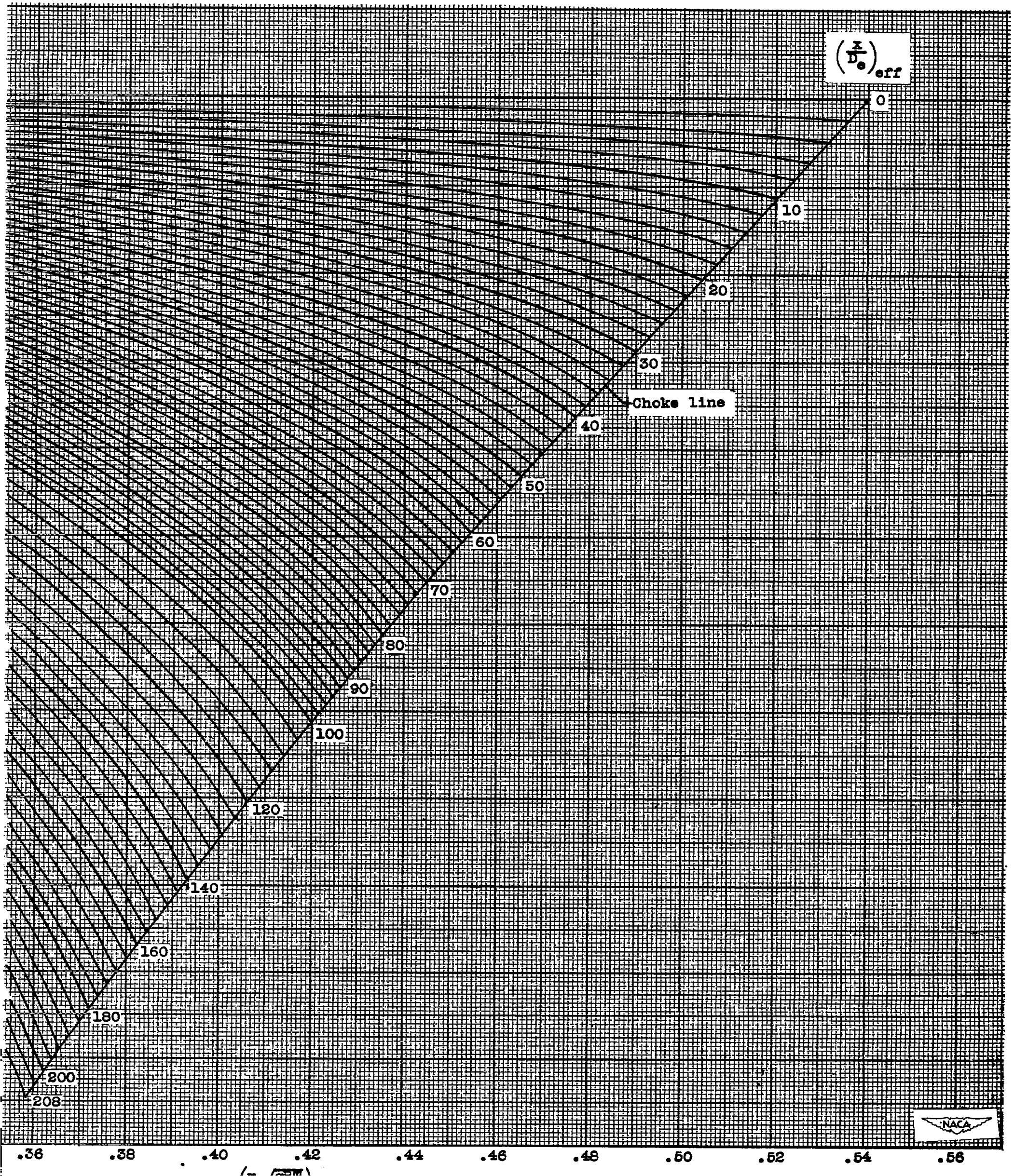
$\left(\frac{x}{D_e}\right)_{eff}$
0
10
20
30
Choke line
40
50
60
70
80
90
100
120
140
160
180
200
208
NACA
.36
.38
.40
.42
.44
.46
.48
.50
.52
.54
.56